

1 **Antiparasitic effect of stilbene and terphenyl compounds against *Trypanosoma***
2 ***cruzi* parasites**

3
4

5 Federica Bruno¹, Germano Castelli^{1*}, Fabrizio Vitale¹, Simone Catanzaro¹, Valeria Vitale Badaco¹,
6 Marinella Roberti², Claudia Colomba³, Antonio Cascio³, Manlio Tolomeo³.

7
8

1 **1** National Reference Center for Leishmaniasis (C.Re.Na.L.), Istituto Zooprofilattico Sperimentale
2 della Sicilia, Via Gino Marinuzzi 3, 90129, Palermo, Italy.

3 **2** Department of Pharmacy and Biotechnology, University of Bologna, Via Belmeloro 6, 40126,
4 Bologna, Italy.

5 **3** Department of Health Promotion Sciences, Section of Infectious Diseases, University of Palermo,
6 Via del Vespro 129, 90127, Palermo, Italy.

7
8
9

10
11

12 * Email corresponding:

13 germano.castelli@izssicilia.it

14
15
16
17
18
19
20
21
22
23
24
25
26

27 **Abstract**

28 **Background.** Chagas disease, also known as American trypanosomiasis, is a potentially life-
29 threatening illness caused by the protozoan parasite *Trypanosoma cruzi*. No progress in the treatment
30 of this pathology has been made since Nifurtimox was introduced more than fifty years ago and is
31 considered very aggressive and may cause several adverse effects. Currently, this drug has severe
32 limitations, including high frequency of undesirable side effects and limited efficacy and availability
33 and the research to discover new drugs for the treatment of Chagas disease is imperative. Many drugs
34 available in the market are natural products as found in nature or compounds designed based on the
35 structure and activity of these natural products.

36
37 **Methodology/Principal Findings.** This study evaluated the in vitro antiparasitic activity in *T.*
38 *cruzi* epimastigotes and intracellular amastigotes of a series of stilbene and terphenyl compounds
39 previously synthesized. The action of the most selective compounds has been investigated by flow
40 cytometry analysis to evaluate the mechanism of cell death. The ability to induce apoptosis or
41 caspase-1 inflammasome were assayed in macrophages infected with *T. cruzi* after treatment
42 comparing with Nifurtimox.

43
44 **Conclusions/Significance.** The stilbene ST18 was the most potent compound of the series. It
45 was slightly less active than Nifurtimox in epimastigotes but most active in intracellular amastigotes.
46 Compared to Nifurtimox, it was markedly less cytotoxic when tested in vitro on normal cells. ST18
47 was able to induce a marked increase of parasites positive to Annexin V and monodansylcadaverine.
48 Moreover, ST18 induced the activation in infected macrophages of caspase-1, a conserved enzyme
49 which plays a main role in controlling parasitemia, host survival, and the onset of adaptive immune
50 response in *Trypanosoma* infection. The antiparasitic activity of ST18 together to its ability to
51 activate caspase-1 in infected macrophages and its low toxicity on normal cells makes this compound
52 interesting for further clinical investigations.

53 **Author Summary**

54

55 Chagas disease is a pathology caused by the protozoan parasite *Trypanosoma cruzi*. No progress
56 in the treatment of this pathology has been made since benznidazole and Nifurtimox were introduced
57 more than fifty years ago. However, these drugs have severe limitations and the research to discover
58 new drugs for the treatment of Chagas disease is imperative. We evaluated the *in vitro* antiparasitic
59 activity in *T. cruzi* epimastigotes of a series of stilbene and terphenyl compounds previously
60 synthesized. The stilbene ST18 was the most potent compound of the series. It was slightly less active
61 than nifurtimox in epimastigotes but most active in intracellular amastigotes. Compared to Nifurtimox,
62 it was markedly less cytotoxic when tested in vitro on normal cells. ST18 was able to induce a marked
63 increase of parasites positive to Annexin V and monodansylcadaverine. Moreover, this compound
64 induced the activation in infected macrophages of caspase-1, an evolutionarily conserved enzyme
65 which plays a main role in controlling parasitemia, host survival, and the onset of adaptive immune
66 response in *T. cruzi* infection. The antiparasitic activity of ST18 together to its ability to activate
67 caspase-1 in infected macrophages and its low toxicity on normal cells makes this compound
68 interesting for further clinical investigations.

69

70

71

72

73

74

75

76

77

78

79 **Introduction**

80 *Trypanosoma cruzi* (*T. cruzi*) is a protozoan parasite transmitted primarily by triatomine insects.
81 It is the agent of Chagas disease, an endemic pathology in Latin America that affects about 6-8 million
82 people worldwide [1] and causes approximately 50,000 deaths per year. Only two nitroheterocyclic
83 drugs, Nifurtimox and benznidazole, are available for the treatment of Chagas disease. Currently,
84 these drugs have severe limitations, including high frequency of undesirable side effects, long
85 protocols of treatment, and limited efficacy and availability; although they are effective for the
86 treatment of acute infections. Experimental toxicity studies with Nifurtimox evidenced neurotoxicity,
87 testicular damage, ovarian toxicity, and deleterious effects in adrenal, colon, oesophageal and
88 mammary tissue which frequently necessitate the cessation of treatment. In the case of benznidazole
89 deleterious effects were observed in adrenals, colon and oesophagus. Both drugs exhibited significant
90 mutagenic effects and were shown to be tumorigenic or carcinogenic in some studies [2,3]. Therefore,
91 natural products have always been a source of a great variety of bioactive molecules, mostly
92 substances from the organism secondary metabolism. Many drugs available in the market are natural
93 products as found in nature or compounds designed based on the structure and activity of these natural
94 products (semi-synthetic or completely synthetic)[4]. Recently, several natural and synthetic stilbene
95 and terphenyl have been studied for their anticancer and leishmanicidal properties [5–8], in particular
96 we evaluated the antileishmanial activity of two compounds, a trans-stilbene derivatives and a
97 terphenyl derivatives, namely trans-1,3-dimethoxy-5-(4-methoxystyryl) benzene (ST18) and 3,4",5-
98 trimethoxy-1,1':2',1"-terphenyl (TR4), presented the best activity and safety profiles [9,10].

99 In the current study we evaluated the *in vitro* antiparasitic activity in *T. cruzi* epimastigotes of
100 a series of *cis*- and *trans*-stilbene derivatives in which a variety of substituents were introduced at
101 position 2', 3' and 4' of the stilbene scaffold while the 3-5dimethoxy motif was maintained.
102 Additionally, we studied a series of terphenyl compounds incorporating a phenyl ring as a bioisosteric
103 substitution of the stilbene alkenyl bridge.

104 We observed that the stilbene ST18 was endowed with potent antiparasitic activity in both *T.*
105 *cruzi* epimastigotes and intracellular *T. cruzi* amastigotes. Compared to Nifurtimox, it was markedly
106 less cytotoxic when tested *in vitro* on normal and differentiated cells. Moreover, this compound
107 induced the activation in infected macrophages of caspase-1, an evolutionarily conserved enzyme
108 which plays a main role for controlling parasitemia, host survival, and the onset of adaptive immune
109 response in *T. cruzi* infection.

110

111 **Materials and Methods**

112 **Parasites cultures**

113 A strain of *T. cruzi* taken by stock archive of the OIE Reference Laboratory National Reference
114 Center for Leishmaniasis (C.Re.Na.L. Palermo, Italy) was cultured in 25 cm² flasks (Falcon) at 25 °C
115 and pH 7.18 in RPMI-PY medium, which consisted of RPMI 1640 (Sigma R0883) supplemented
116 with equal volume of Pepton-yeast medium, 10% fetal bovine serum (FBS), 1% glutamine, 250
117 µg/mL gentamicin and 500 µg/mL of 5-fluorocytosine [11].

118

119 **Compounds and sample preparation**

120

121 Compounds ST18 and 6 were synthesized as reported by Kim et al. [12]; compounds 1-5 and
122 8-10 were prepared as previously described by us [6], compounds 7, TR4 and 13-14 were prepared
123 as previously described by us [7], 15 was synthesized as reported by Pizzirani et al. [5]. The purity of
124 compound was determined by elemental analyses and was $\geq 97\%$. Each compound was dissolved in
125 dimethyl sulfoxide (DMSO) in a stock solution at a concentration of 20 mM, stored at -20°C and protected
126 from light. In each experiment DMSO never exceeded 0.2% and this percentage did not interfere with cell
127 growth. Nifurtimox was obtained from Merck Sigma-Aldrich (Milano, Italy).

128

129

130 **Epimastigotes viability assay**

131 To evaluate the effects of compounds in cultures of *T. cruzi* a viability assay protocol similar
132 to that described by Castelli et al. [9] was used with some modifications. Exponentially growing of
133 *T. cruzi* were dispensed at the concentration of 4×10^6 /mL in 25-m² flasks (Falcon) and treated with
134 increasing concentrations (from 1 to 200 μ M) of each compound. After 72 h of treatment the parasites
135 were centrifugated and resuspended in 1 ml of RPMI-PY medium. The suspension of *T. cruzi* from
136 each treatment was mixed with 0.4% trypan blue solution at a ratio of 3:1 (vol/vol). The percentage
137 of vitality of *T. cruzi* was observed by counting in a Bürker hemocytometer for enumeration of stained
138 and unstained cells, taken respectively as dead and living cells, in comparison with the control culture
139 (100% viability). IC₅₀ (half maximal inhibitory concentration) was evaluated after 72 h and was
140 calculated by regression analysis (GraphPad software).

141

142 **Effects of compounds in intracellular amastigotes**

143 U937 monocytic cells (1×10^5 cells/mL) in the logarithmic phase of growth were plated onto
144 chamber Lab Tek culture slides in 2.5 mL of RPMI 1640 (Sigma), 10% FBS medium containing 25
145 ng/mL of phorbol 12-myristate 13-acetate (Sigma) for 18 h to induce macrophage differentiation.

146 After incubation, the medium was removed by washing twice with RPMI-1640 medium. Non
147 adherent cells were removed, and the macrophages were further incubated overnight in RPMI 1640
148 medium supplemented with 10% FBS. Then adherent macrophages were infected with *T. cruzi*
149 epimastigotes at a parasite/macrophage ratio of 50:1 for 24 h at 37 °C in 5% CO₂. Free epimastigotes
150 were removed by three extensive washing with RPMI 1640 medium, and infected macrophages were
151 either incubated 48 h in media alone (control) or with Nifurtimox, ST18 or TR4. With the aim of stain
152 intracellular amastigotes, cells were fixed with iced methanol to permeabilize cell membrane to
153 ethidium bromide and stained with 100 μ g/mL ethidium bromide. The number of amastigotes was
154 determined by examining three coverslips for each treatment. At least 200 macrophages were counted
155 by visual examination under 400 \times magnifications by using a fluorescence microscope Nikon Eclipse

156 E200 (Nikon Instruments Europe, Amsterdam, Netherlands) equipped with a green filter to determine
157 the number of intracellular amastigotes. The number of intracellular amastigotes in samples treated
158 with each compound was expressed as percentage of the untreated control.

159

160 **Mammalian cell cytotoxicity**

161 Potential cytotoxic action of each compound was checked by 3-(4,5-dimethylthiazol-2-yl)-2,5-
162 diphenylterazolium bromide (MTT) assay on macrophages derived by U937 cells and in primary
163 epithelial cells of Cercopithecus (CPE). Macrophages and CPE cells were cultured in RPMI 1640
164 (Sigma) supplemented with 10% fetal bovine serum (FBS, Gibco), penicillin (100 IU/mL) and
165 streptomycin (100 mg/mL). Cells were grown at 37 °C in 5% CO₂ and passaged twice a week. In
166 each experiment, cells (10⁵/well) were incubated into 96-well plates overnight in a humidified 5%
167 CO₂ atmosphere at 37 °C to ensure cell adherence. After 24 h, cells were treated with increasing
168 concentrations of each compound. Non-treated cells were included as a negative control. After 72 h
169 incubation with each compound, the MTT (5 mg/mL) was added to each well and incubated at 37 °C
170 for 4 h. Then the medium and MTT were removed, cells washed by PBS and 200 µL of DMSO were
171 added to dissolve the formazan crystals. The absorbance was measured using a microplate reader
172 Spectrostar Nano (BMG LabTech) at 570 nm. The reduction of MTT to insoluble formazan was done
173 by the mitochondrial enzymes of viable cells and so is an indicator of cell viability. Therefore,
174 decreases of absorbance indicate toxicity to the cell. The viability was calculated using the following
175 formula: $[(L2/L1) \times 100]$, where L1 is the absorbance of control cells and L2 is the absorbance of
176 treated cells. The IC₅₀ was calculated by regression analysis (GraphPad software).

177 The selectivity index (SI) was determined by dividing the IC₅₀ calculated in mammalian cells
178 and the IC₅₀ calculated in *T. cruzi* parasites.

179

180 **Cell cycle analysis by flow cytometry**

181 Epimastigotes (4×10^6) were incubated for 48 h with each compounds at 26 °C. Afterward,
182 parasites were washed 3 times with PBS containing 0.02 M EDTA to avoid clumps and were then
183 fixed with cold methanol for 24 h. The parasites were resuspended in 0.5 mL of PBS containing
184 RNase I (50 µg/mL) and PI (25 µg/mL) and were then incubated at 25 °C for 20 min. The material
185 was kept on ice until analysis. The stained parasites were analysed in single-parameter frequency
186 histograms by using a FACScan flow cytometer (Becton Dickinson, CA).

187

188 **Cell volume determination**

189 Epimastigotes were collected by centrifugation at 1,000g, washed twice in PBS, resuspended
190 in PBS to 500×10^3 parasites/mL, and analysed by FACScan flow cytometer (Becton Dickinson, CA).
191 Density plots of forward (FSC) versus side (SSC) scatter represent the acquisition of 10×10^3 events.

192

193 **Determination of apoptosis by Annexin V**

194 Externalization of phosphatidylserine on the outer membrane of parasites with and without
195 treatment was determined by using Annexin V labeling kit following the manufacturer's protocol
196 (Annexin-V-FITC Apoptosis Detection Kit Alexis, Switzerland). Briefly, epimastigotes (2×10^6) were
197 washed with PBS and centrifuged at 500 g for 5 min. The pellet was suspended in 100 µL of staining
198 solution containing FITC-conjugated Annex-in-V and propidium iodide (Annexin-V-Fluos Staining
199 Kit, Roche Molecular Biochemicals, Germany) and incubated for 15 min at 20 °C. Annexin V
200 positive parasites were determined by using a FACScan flow cytometer (Becton Dickinson, CA).

201

202 **Monodansylcadaverine labelling**

203 Monodansylcadaverine (MDC), which is an autofluorescent compound due to the dansyl
204 residue conjugated to cadaverine, have been shown to accumulate in acidic autophagic vacuoles. The
205 concentration of MDC in autophagic vacuole is the consequence of an ion-trapping mechanism and
206 an interaction with lipids in autophagic vacuoles (autophagic vacuoles are rich in membrane lipids).

207 The use of MDC staining is a rapid and convenient approach to assay autophagy, as shown in cultured
208 cells [13]. Autophagic vacuoles were labeled with MDC by incubating cells on coverslips with 0.05
209 mM MDC in PBS at 37°C for 10 minutes. After incubation, cells were washed four times with PBS
210 and immediately analysed by fluorescence microscopy (Nikon Eclipse E 200, Japan) equipped with
211 a blue filter. Images were obtained with a Nikon Digital Sight DS-SM (Nikon, Japan) camera and
212 processed using the program EclipseNet, version 1.20.0 (Nikon, Japan).

213

214 **Caspase-1 detection**

215 To evaluate the level of active caspase-1, U937 cell line in macrophagic form infected with *T.*
216 *cruzi* was used. Infected macrophages were incubated for 24 h at 37 °C in 5% CO₂. Free parasites
217 were removed by extensive washing with RPMI-1640 medium, and infected cells were either
218 incubated in media alone (infection control) or with each compound. After 48h, the culture medium
219 was removed and treated with caspase-1 assay kit (Promega) following the manufacturer's
220 instructions.

221

222 **Statistical analysis**

223 All assays were performed by two observers in three replicates samples and repeated with three
224 new batches of parasites. The mean and standard error of at least three experiments were determined.
225 The differences between the mean values obtained for experimental groups were evaluated by the
226 Student's t test. P-values of 0.05 or less were considered significant. All statistical analysis was
227 performed using GraphPad Prism 5 software. The IC₅₀ values were calculated by linear regression.

228

229 **Results**

230 ***Anti-Trypanosoma cruzi* activity**

231 Table 1 shows the *in vitro* antiparasitic effects evaluated as IC₅₀ of different stilbenes (ST18, 1-
232 10) and terphenyls (TR4, 11-15) in *T. cruzi* epimastigotes. These compounds were previously

233 synthesized by us except ST18 and 6 that were reported by Kim et al. [12]. Data were compared to
234 those obtained with Nifurtimox which is the drug currently used for the treatment of *T. cruzi* infection.
235 The most active compounds of the series were the stilbene ST18 (IC₅₀ = 4.6 μM) and the terphenyl
236 TR4 (IC₅₀ = 30 μM).

237 Figure 1A shows the *in vitro* effects of Nifurtimox, ST18 and TR4 used at increasing
238 concentrations for 72 h in *T. cruzi* epimastigotes. ST18 was markedly more potent than TR4 but less
239 active than Nifurtimox. Upon entering the mammalian host, *T. cruzi* parasites transform into the
240 amastigote stage that reside inside the phagolysosomal vacuoles of macrophages. We evaluated the
241 anti-amastigote efficacy in differentiated macrophage cells (derived from U937 cells) infected with
242 *T. cruzi* as reported in material and methods. Infected macrophages were treated with Nifurtimox,
243 ST18 and TR4 used at increasing concentrations for 72 h. Differently from the results obtained in
244 epimastigotes, the anti-parasitic effect of ST18 in infected macrophages was higher than that observed
245 using Nifurtimox (Fig. 1B).

246

247 **Fig 1. Effects of compounds Nifurtimox, ST18 and TR4 in *Trypanosoma cruzi* epimastigotes and**
248 **intracellular amastigotes. (A)** Number of viable *T. cruzi* epimastigotes expressed as percentage of
249 untreated control after 72 h exposure to increasing concentrations of Nifurtimox, ST18 and TR4. **(B)**
250 Number of intracellular amastigotes expressed as percentage of the untreated control after 72 h
251 treatment with Nifurtimox, ST18 and TR4. Bars indicate the mean ± SE from four independent
252 experiments. Data obtained are statistically significant at P < 0.05.

253

254 **Mammalian cell cytotoxicity and SI**

255 Primary epithelial cells of Cercopithecus (CPE) and macrophages derived by differentiation of
256 U937 cells were treated with increasing concentrations of ST18 and Nifurtimox. Cytotoxicity was
257 evaluated after 72 h through MTT assay. ST18 showed a very low cytotoxicity in both cell lines
258 compared to Nifurtimox (Fig. 2A) In macrophages the IC₅₀ of ST18 was 143 μM while the IC₅₀ of

259 Nifurtimox was 28 μ M with a SI of 31 for ST18 and 8.75 for Nifurtimox. In CPE the IC50s of ST18
260 and Nifurtimox were 155 μ M and 77 μ M respectively with a SI of 33.7 for ST18 and 24 for
261 Nifurtimox. (Fig. 2B)

262

263

264 **Fig 2. Cytotoxic effects of compounds ST18 and Nifurtimox in Mammalian cells. (A)** Cytotoxic
265 effects of compounds ST18 and Nifurtimox in primary epithelial cells of Cercopithecus (CPE). **(B)**
266 Cytotoxic effects of compounds ST18 and Nifurtimox in U937 macrophage cells. Bars indicate the
267 mean \pm SE from four independent experiments. Data obtained are statistically significant at $P < 0.05$.

268

269 **Cell cycle**

270 The effects of Nifurtimox, ST18 and TR4 on cell cycle distribution of *T. cruzi* was analysed by
271 FACScan flow cytometer. To exclude in the study of cell cycle dead cells that are often located in a
272 sub-G0-G1 peak we decided to study the effects of each compound on the cell cycle by treating the
273 parasites for a period of time and with concentrations of each compound that caused a block of cell
274 growth (evaluated by counting parasites on a hemocytometer) without causing a relevant number of
275 dead cells (evaluated by trypan blue staining). Since after 72 h of treatment the cell growth inhibition
276 was associated to an increase in cell death number (data not shown) we studied the effects of each
277 compound on cell cycle after only 48 h of drug exposure treating parasites with 35 μ M Nifurtimox,
278 50 μ M ST18 and 90 μ M TR4. This treatment caused a complete block of cell growth with a
279 percentage of dead cells lower than 10%. Cell cycle distribution was analysed by the standard
280 propidium iodide procedure. Nifurtimox did not determined important variations in cell cycle
281 distribution, but only a little reduction in the G2M peak. In contrast, ST18 caused an evident block
282 in G2M while TR4 a block in G1 (Fig 3).

283

284 **Fig 3. Effects of Nifurtimox, ST18 and TR4 on DNA content/parasite in *Trypanosoma cruzi***
285 **epimastigotes.** The parasites were cultured without compound (control, panel a) or with 35 μ M of
286 Nifurtimox (panel b), 50 μ M of ST18 (panel c) and 90 μ M of TR4 (panel d). Cell cycle distribution
287 was analysed by the standard propidium iodide procedure. G1, S, and G2–M cells are indicated in
288 panel a.

289

290 **Physical parameters**

291 We studied the physical parameters of *T. cruzi* parasites treated with Nifurtimox, ST18 and TR4
292 by FACScan flow cytometer as previously reported by Jimenez et al [14]. Figure 4A shows density
293 plots for forward scatter (FSC) versus side scatter (SSC) in *T. cruzi* epimastigotes untreated or treated
294 with with 35 μ M Nifurtimox, 50 μ M ST18, and 90 μ M TR4 for 72 h. The measurement of forward
295 scatter allows for the discrimination of cells by size. FSC intensity is proportional to the diameter of
296 the cell. Side scatter measurement provides information about the internal complexity (i.e. granularity)
297 of a cell. The analysis of the density plot of Trypanosome epimastigotes treated with Nifurtimox
298 shows a marked reduction in the average cell size compared to the control. In contrast, FACS analysis
299 of Trypanosome epimastigotes treated with ST18 shows a heterogeneous population characterized by
300 parasites with low dimension and parasites with increased size and granularity. No important
301 modifications were observed with TR4. These data were confirmed by the FACS histograms as shown
302 in Figure 4B.

303

304

305 **Fig 4. FACS analysis of *Trypanosoma cruzi* epimastigotes cell volume populations. (A)** Forward
306 light scatter (FSC-H) was considered as function of cell size and side light scatter (SSC-H) as result
307 of cell granularity. Density plots for FSC versus SSC in *T. cruzi* epimastigotes after 72 h treatment
308 with Nifurtimox (panel b), ST18 (panel c) and TR4 (panel d). Untreated control is represented in
309 panel a. **(B)** Representative FACS histogram showing FSC-H and SSC-H of *T. cruzi* epimastigotes

310 after 72 h treatment with Nifurtimox (panels a and d) ST18 (panels b and e) and TR4 (panels c and
311 f). Thin line: No treated control parasites; thick line: parasites treated with each compound. Data are
312 representative of three separate experiments.

313

314 **Annexin V and MDC labeling**

315 The loss of cell volume or cell shrinkage is a hallmark of the early phase of the apoptotic process.
316 In order to confirm whether volume reduction of parasites was related to apoptosis, the exposition of
317 phosphatidylserine at the cell surface was analysed by Annexin V labeling test after treatment with
318 Nifurtimox, ST18 and TR4. A significant increase in the percentage of parasites positive to Annexin
319 V was observed after treatment with Nifurtimox and, to a lesser extent, after treatment with ST18
320 (Fig. 5).

321

322 **Fig 5. Analysis of phosphatidylserine (PS) extracellular exposure.** Representative dot plot of
323 FACS analysis for PS exposure, measured by double staining with Annexin V-FITC and propidium
324 iodide (PI) in *T. cruzi* epimastigotes after 72 h treatment with Nifurtimox (panel b) and ST18 (panel
325 c) and TR4 (panel d). No treated control is represented in panel a. Lower left quadrant belongs to
326 control cells (Annexin V negative/PI negative), lower right quadrant belongs to early apoptotic cells
327 (Annexin V positive/PI negative), upper right quadrant belongs to late apoptotic cells (Annexin V
328 positive/PI positive), upper left quadrant belongs to necrotic cells (Annexin V negative/PI positive).
329 Data are representative of three separate experiments.

330

331 Since the analysis of physical parameters of *T. cruzi* treated with ST18 showed also a cell
332 population with increased size and granularity, parameters that are hallmarks of the autophagic
333 process, parasites were treated with monodansylcadaverine (MDC), a specific fluorescent marker for
334 autophagic vacuoles [15]. About 30% of parasites treated 72 h with 40 μ M ST18 were strongly
335 positive to MDC test showing numerous fluorescent vacuoles in the cytoplasm. These vacuoles were

336 not observed in untreated control and in samples treated with Nifurtimox or TR4 (data not shown)
337 (Fig. 6).

338

339 **Fig 6. Autophagic induction by ST18 in *Trypanosoma cruzi* epimastigotes.** Parasites were
340 incubated with 0.05 mM MDC in PBS at 37 ° C for 10 minutes and observed in a fluorescent
341 microscope Nikon Eclipse E 200 (100x). A and b: Control. c and d: *T. cruzi* epimastigotes treated 72
342 h with 40 µM ST18. Eclipse E 200 (100x). a and b: Control. c and d: *T. cruzi* epimastigotes treated 72
343 h with 40 µM ST18.

344

345 **Caspase-1**

346 Infection with *T. cruzi* results in activation of caspase-1 and inflammasome formation.
347 Inflammasome is indispensable for controlling parasitemia, host survival, and the onset of adaptive
348 immune response [16]. In this sense, inflammasome activation is fully dependent on caspase-1. We
349 evaluated the levels of active caspase-1 in U937 macrophages infected with *T. cruzi* after treatment
350 with Nifurtimox, ST18 and TR4. In macrophages infected with trypanosomes and treated with ST18
351 spectrophotometric analysis showed a substantial increase in active caspase-1 compared to the control.
352 In contrast no increase in caspase-1 was observed in samples of infected macrophages treated with
353 Nifurtimox or TR4 and in uninfected macrophages treated with ST18. (Fig. 7).

354

355 **Fig 7. Caspase-1 activity.** Levels of active caspase-1 in U937 macrophages infected with in *T. cruzi*
356 epimastigotes after 48 hours of treatment with 50 µM of ST18, TR4 and Nifurtimox (Nfx). C =
357 untreated control. Bars indicate the mean ± SE from four independent experiments. *p<0.05 vs
358 control.

359

360 **Discussion**

361 We evaluated the *in vitro* antiparasitic effects in *T. cruzi* epimastigotes of a series of *cis*- and
362 *trans*-stilbenes bearing 3,5-dimethoxy motif at A phenyl ring and amino, methoxy and hydroxyl
363 function at 2', 3'- and/or 4'-position at B phenyl ring. Moreover, in an attempt to increase the
364 chemical diversity of the compounds we studied a small series of terphenyl derivatives that notably
365 do not bear the ethylene double bond that is the main reason for the chemical and metabolic instability
366 of stilbenes [17,18]. Data were compared to those obtained with Nifurtimox which is the drug
367 currently used for the treatment of Trypanosome infections. Among the stilbene series, ST18 bearing
368 a 4'-methoxy function was the most active compound showing an $IC_{50} = 4.6 \mu M \pm 0.4$. Regarding
369 the terphenyl derivatives the best results were obtained with the trimethoxylated compound TR4
370 ($IC_{50} = 30 \pm 4.3$) that is the *orto*-terphenyl analogue of ST18. Nifurtimox was more active than ST18
371 in *T. cruzi* epimastigotes but less active in intramacrophagic *T. cruzi* amastigotes.

372 The most interesting data observed in this study was the difference in the selectivity index value
373 between ST18 and Nifurtimox. Nifurtimox is a drug with several adverse effects including mutagenic
374 and tumorigenic effects [3]. ST18 has been described in the literature by different names, including
375 resveratrol trimethyl ether (RTE) [19,20], MR-3 [21,22], M-5 [23], BTM-0521 [24], trimethoxy
376 resveratrol [25], trimethylated resveratrol [26] and TMS [20,27]. It is a natural stilbene isolated from
377 *Virola cuspidata* and *Virola elongata* bark [27,28]. Natural stilbenes have received increasing
378 attention due to their potent antioxidant properties and their marked effects in the prevention of
379 various oxidative stress associated diseases such as cancer [28]. A number of clinical trials using
380 natural stilbenes such as resveratrol and pterostilbene have shown that they are therapeutically
381 effective and pharmacologically safe because it showed no organ-specific or systemic toxicity [29–
382 33]. Preclinical pharmacokinetic studies have shown that ST18 has appropriate pharmacokinetic
383 profiles that make it a promising drug candidate for further pharmaceutical development [19]. It
384 exhibited anti-proliferative and/or apoptosis-inductive activities in various cancer cells with a potency
385 usually higher than resveratrol [20,23,34–36]. Moreover it has shown anti-inflammatory [37–40],
386 gastro protective [41], and hepato-protective activities [26]. Here, we have demonstrated that ST18

387 showed a very low toxicity on normal and differentiated cells and the SI tested in *T. cruzi* parasites
388 was higher than that calculated for Nifurtimox.

389 Several studies have shown that Nifurtimox induces production of reactive oxygen species
390 (ROS) and subsequent apoptosis in neoplastic cells [42–44]. Although programmed cell death is very
391 controversial in unicellular eukaryotes we observed that Nifurtimox caused a marked reduction in the
392 average cell size of *T. cruzi* epimastigotes and a significant increase in the percentage of parasites
393 positive to Annexin V. This compound did not cause in parasites an increase of MDC, an important
394 marker of autophagy. In contrast ST18 produced a heterogeneous population characterized by
395 parasites with low dimension and parasites with increased size and granularity. ST18 induced an
396 increase of both Annexin V and MDC positive parasites.

397 Several works have reported the activation of autophagic process in Trypanosomatids during
398 starvation responses and life cycle developments. Moreover, endoplasmic reticulum (ER) stress and
399 anti-parasitic drugs can induce autophagy in *T. brucei* and *T. cruzi* [45–47]. In our experiments ST18
400 caused in *T. cruzi* both phosphatidylserine expression and dansylcadaverina staining suggesting that
401 this compound could be capable to activate both apoptosis and autophagy.

402 Lim et al. [48] have obtained similar results in *T. brucei rhodesiense* using two piperidine alkaloids,
403 (+)-spectaline and iso-6-spectaline. These compounds caused the formation of autophagic vacuoles
404 were to monodansylcadaverine staining indicating the activation of the autophagic process. When
405 trypanosomes were treated with piperidine alkaloids for 72 h they showed apoptotic aspects including
406 phosphatidylserine exposure.

407 Several studies have demonstrated that autophagy and apoptosis communicate with each other to
408 decides the fate of the cell during physiological and pathological conditions [49]. It has been supposed
409 that, after the activation of stress or drug induced autophagy, when the stress condition increases
410 towards a point of no return cells block autophagy and activate programmed cell death. Of interest,
411 the analysis of cell cycle showed that both Nifurtimox and TR4 caused a decrease of parasites in G2M
412 phase of cell cycle while ST18 determined an important block in G2M. A correlation between G2M

413 block and autophagy activation has been observed in different experimental models but the precise
414 mechanism by which microtubule targeting agents induce autophagic cell death is not known [50–
415 53].

416 Finally, we observed that ST18, but not TR4 and Nifurtimox, induced a marked increase of
417 active caspase-1 in *T. cruzi* infected macrophages. The capability of ST18 to activate caspase-1 in *T.*
418 *cruzi* infected macrophages may, in part, explain the greater antiparasitic effect of ST18 than
419 Nifurtimox in intramacrophagic trypanosomes. In fact, Yu et al. [54] demonstrated that canonical
420 inflammasome activation triggers ROS production in macrophages in a caspase-1-dependent manner.
421 Reactive oxygen species (ROS) protect the host against a large number of pathogenic microorganisms
422 including trypanosome [55,56].

423 In conclusion, after testing 17 different compounds designed and synthesized previously by us,
424 we selected a stilbene compound, ST18, endowed with a potent antiparasitic activity in *T. cruzi*
425 epimastigotes and intracellular amastigotes. The antiparasitic activity of ST18 together to its ability
426 to activate caspase-1 in infected macrophages and its low toxicity on normal cells makes this
427 compound interesting for further biological and clinical studies in *T. cruzi*.

428

429 **Acknowledgments**

430 This work is supported by grants from ‘Istituto Zooprofilattico Sperimentale della Sicilia’,
431 Palermo, Italy code number: RC IZS SI 05/16.

432

433 **References**

434

- 435 1. Shoemaker EA, Dale K, Cohn DA, Kelly MP, Zoerhoff KL, Batcho WE, et al. Gender and
436 neglected tropical disease front-line workers: Data from 16 countries. *PloS One*. 2019;14:
437 e0224925. doi:10.1371/journal.pone.0224925
- 438 2. Urbina, J. A., and R. Docampo. Specific chemotherapy of Chagas disease: controversies and
439 advances. *Trends Parasitol*. 2003.

- 440 3. Castro JA, de Mecca MM, Bartel LC. Toxic side effects of drugs used to treat Chagas' disease
441 (American trypanosomiasis). *Hum Exp Toxicol.* 2006;25: 471–479.
442 doi:10.1191/0960327106het653oa
- 443 4. Morais TR, Conserva GAA, Varela MT, Costa-Silva TA, Thevenard F, Ponci V, et al.
444 Improving the drug-likeness of inspiring natural products - evaluation of the antiparasitic
445 activity against *Trypanosoma cruzi* through semi-synthetic and simplified analogues of licarin
446 A. *Sci Rep.* 2020;10: 5467. doi:10.1038/s41598-020-62352-w
- 447 5. Pizzirani D, Roberti M, Cavalli A, Grimaudo S, Di Cristina A, Pipitone RM, et al.
448 Antiproliferative Agents That Interfere with the Cell Cycle at the G1 → S Transition: Further
449 Development and Characterization of a Small Library of Stilbene-Derived Compounds.
450 *ChemMedChem.* 2008;3: 345–355. doi:10.1002/cmdc.200700258
- 451 6. Roberti M, Pizzirani D, Simoni D, Rondanin R, Baruchello R, Bonora C, et al. Synthesis and
452 biological evaluation of resveratrol and analogues as apoptosis-inducing agents. *J Med Chem.*
453 2003;46: 3546–3554. doi:10.1021/jm030785u
- 454 7. Roberti M. Identification of a Terphenyl Derivative that Blocks the Cell Cycle in the G0–G1
455 Phase and Induces Differentiation in Leukemia Cells | *Journal of Medicinal Chemistry.* 2006
456 [cited 2 Feb 2021]. Available: <https://pubs.acs.org/doi/pdf/10.1021/jm060253o>
- 457 8. Tolomeo M, Roberti M, Scapozza L, Tarantelli C, Giacomini E, Titone L, et al. TTAS a new
458 stilbene derivative that induces apoptosis in *Leishmania infantum*. *Exp Parasitol.* 2013;133: 37–
459 43. doi:10.1016/j.exppara.2012.10.006
- 460 9. Castelli G, Bruno F, Vitale F, Roberti M, Colomba C, Giacomini E, et al. In vitro antileishmanial
461 activity of trans-stilbene and terphenyl compounds. *Exp Parasitol.* 2016;166: 1–9.
462 doi:10.1016/j.exppara.2016.03.007
- 463 10. Bruno F, Castelli G, Vitale F, Giacomini E, Roberti M, Colomba C, et al. Effects of trans-
464 stilbene and terphenyl compounds on different strains of *Leishmania* and on cytokines
465 production from infected macrophages. *Exp Parasitol.* 2018;184: 31–38.
466 doi:10.1016/j.exppara.2017.11.004
- 467 11. Castelli G, Galante A, Lo Verde V, Migliazzo A, Reale S, Lupo T, et al. Evaluation of two
468 modified culture media for *Leishmania infantum* cultivation versus different culture media. *J*
469 *Parasitol.* 2014;100: 228–230. doi:10.1645/13-253.1
- 470 12. Kim S, Ko H, Park JE, Jung S, Lee SK, Chun Y-J. Design, synthesis, and discovery of novel
471 trans-stilbene analogues as potent and selective human cytochrome P450 1B1 inhibitors. *J Med*
472 *Chem.* 2002;45: 160–164. doi:10.1021/jm010298j
- 473 13. Munafó DB, Colombo MI. A novel assay to study autophagy: regulation of autophagosome
474 vacuole size by amino acid deprivation. *J Cell Sci.* 2001;114: 3619–3629.
- 475 14. V J, R P, Ma S, N G. Natural programmed cell death in *T. cruzi* epimastigotes maintained in
476 axenic cultures. In: *Journal of cellular biochemistry* [Internet]. 15 Oct 2008 [cited 15 Feb 2021].
477 doi:10.1002/jcb.21864
- 478 15. Biederbick A, Kern HF, Elsässer HP. Monodansylcadaverine (MDC) is a specific in vivo marker
479 for autophagic vacuoles. *Eur J Cell Biol.* 1995;66: 3–14.

- 480 16. paroli. *Frontiers | NLRP3 Inflammasome and Caspase-1/11 Pathway Orchestrate Different*
481 *Outcomes in the Host Protection Against Trypanosoma cruzi Acute Infection | Immunology.*
482 [cited 2 Feb 2021]. Available:
483 <https://www.frontiersin.org/articles/10.3389/fimmu.2018.00913/full>
- 484 17. Metzler, M. Metabolic activation of diethylstilbestrol: Indirect evidence for the formation of a
485 stilbene oxide intermediate in hamster and rat. *Biochem Pharmacol.* 1975;24: 1449–1453.
486 doi:10.1016/0006-2952(75)90373-1
- 487 18. Neumann HG, Metzler M, Töpner W. Metabolic activation of diethylstilbestrol and
488 aminostilbene-derivatives. *Arch Toxicol.* 1977;39: 21–30. doi:10.1007/BF00343272
- 489 19. Hs L, Pc H. Preclinical pharmacokinetic evaluation of resveratrol trimethyl ether in sprague-
490 dawley rats: the impacts of aqueous solubility, dose escalation, food and repeated dosing on oral
491 bioavailability. In: *Journal of pharmaceutical sciences* [Internet]. Oct 2011 [cited 15 Feb 2021].
492 doi:10.1002/jps.22588
- 493 20. Tt W, Nw S, Ys K, Cs M, Am R. Differential effects of resveratrol and its naturally occurring
494 methylether analogs on cell cycle and apoptosis in human androgen-responsive LNCaP cancer
495 cells. In: *Molecular nutrition & food research* [Internet]. Mar 2010 [cited 15 Feb 2021].
496 doi:10.1002/mnfr.200900143
- 497 21. Cj W, Yt Y, Ct H, Gc Y. Mechanisms of apoptotic effects induced by resveratrol,
498 dibenzoylmethane, and their analogues on human lung carcinoma cells. In: *Journal of*
499 *agricultural and food chemistry* [Internet]. 24 Jun 2009 [cited 15 Feb 2021].
500 doi:10.1021/jf900531m
- 501 22. Yt Y, Cj W, Ct H, Gc Y. Resveratrol analog-3,5,4'-trimethoxy-trans-stilbene inhibits invasion
502 of human lung adenocarcinoma cells by suppressing the MAPK pathway and decreasing matrix
503 metalloproteinase-2 expression. In: *Molecular nutrition & food research* [Internet]. Mar 2009
504 [cited 15 Feb 2021]. doi:10.1002/mnfr.200800123
- 505 23. Bader Y, Madlener S, Strasser S, Maier S, Saiko P, Stark N, et al. Stilbene analogues affect cell
506 cycle progression and apoptosis independently of each other in an MCF-7 array of clones with
507 distinct genetic and chemoresistant backgrounds. *Oncol Rep.* 2008;19: 801–810.
508 doi:10.3892/or.19.3.801
- 509 24. Lu M, Liu B, Xiong H, Wu F, Hu C, Liu P. Trans-3,5,4'-trimethoxystilbene reduced gefitinib
510 resistance in NSCLCs via suppressing MAPK/Akt/Bcl-2 pathway by upregulation of miR-345
511 and miR-498. *J Cell Mol Med.* 2019;23: 2431–2441. doi:10.1111/jcmm.14086
- 512 25. Sj D, K L, Am R, S D, Cs M, Ad P, et al. Trimethoxy-resveratrol and piceatannol administered
513 orally suppress and inhibit tumor formation and growth in prostate cancer xenografts. In: *The*
514 *Prostate* [Internet]. Aug 2013 [cited 15 Feb 2021]. doi:10.1002/pros.22657
- 515 26. H R, M S, V T, V P-A, P M. Resveratrol and trimethylated resveratrol protect from acute liver
516 damage induced by CCl₄ in the rat. *J Appl Toxicol JAT.* 2008;28: 147–155.
517 doi:10.1002/jat.1260
- 518 27. B L, Xj L, Zb Y, Jj Z, Tb L, Xj Z, et al. Inhibition of NOX/VPO1 pathway and inflammatory
519 reaction by trimethoxystilbene in prevention of cardiovascular remodeling in hypoxia-induced
520 pulmonary hypertensive rats. In: *Journal of cardiovascular pharmacology* [Internet]. Jun 2014
521 [cited 15 Feb 2021]. doi:10.1097/FJC.0000000000000082

- 522 28. Sirerol JA, Rodríguez ML, Mena S, Asensi MA, Estrela JM, Ortega AL. Role of Natural
523 Stilbenes in the Prevention of Cancer. *Oxid Med Cell Longev*. 2016;2016: 3128951.
524 doi:10.1155/2016/3128951
- 525 29. Almeida L, Vaz-da-Silva M, Falcão A, Soares E, Costa R, Loureiro AI, et al. Pharmacokinetic
526 and safety profile of trans-resveratrol in a rising multiple-dose study in healthy volunteers. *Mol*
527 *Nutr Food Res*. 2009;53 Suppl 1: S7-15. doi:10.1002/mnfr.200800177
- 528 30. la Porte C, Voduc N, Zhang G, Seguin I, Tardiff D, Singhal N, et al. Steady-State
529 pharmacokinetics and tolerability of trans-resveratrol 2000 mg twice daily with food, quercetin
530 and alcohol (ethanol) in healthy human subjects. *Clin Pharmacokinet*. 2010;49: 449–454.
531 doi:10.2165/11531820-000000000-00000
- 532 31. Boocock DJ, Faust GES, Patel KR, Schinas AM, Brown VA, Ducharme MP, et al. Phase I Dose
533 Escalation Pharmacokinetic Study in Healthy Volunteers of Resveratrol, a Potential Cancer
534 Chemopreventive Agent. *Cancer Epidemiol Prev Biomark*. 2007;16: 1246–1252.
535 doi:10.1158/1055-9965.EPI-07-0022
- 536 32. Brown VA, Patel KR, Viskaduraki M, Crowell JA, Perloff M, Booth TD, et al. Repeat dose
537 study of the cancer chemopreventive agent resveratrol in healthy volunteers: safety,
538 pharmacokinetics, and effect on the insulin-like growth factor axis. *Cancer Res*. 2010;70: 9003–
539 9011. doi:10.1158/0008-5472.CAN-10-2364
- 540 33. Patel KR, Brown VA, Jones DJL, Britton RG, Hemingway D, Miller AS, et al. Clinical
541 pharmacology of resveratrol and its metabolites in colorectal cancer patients. *Cancer Res*.
542 2010;70: 7392–7399. doi:10.1158/0008-5472.CAN-10-2027
- 543 34. D S, M R, Fp I, E A, S A, P M, et al. Stilbene-based anticancer agents: resveratrol analogues
544 active toward HL60 leukemic cells with a non-specific phase mechanism. In: *Bioorganic &*
545 *medicinal chemistry letters* [Internet]. 15 Jun 2006 [cited 15 Feb 2021].
546 doi:10.1016/j.bmcl.2006.03.028
- 547 35. V C, R C, L L, S S, C S, C T. Antiproliferative activity of methylated analogues of E- and Z-
548 resveratrol. In: *Zeitschrift fur Naturforschung. C, Journal of biosciences* [Internet]. Apr 2007
549 [cited 15 Feb 2021]. doi:10.1515/znc-2007-3-406
- 550 36. Pan M-H, Gao J-H, Lai C-S, Wang Y-J, Chen W-M, Lo C-Y, et al. Antitumor activity of 3,5,4'-
551 trimethoxystilbene in COLO 205 cells and xenografts in SCID mice. *Mol Carcinog*. 2008;47:
552 184–196. doi:10.1002/mc.20352
- 553 37. Yuan Q, Peng J, Liu S-Y, Wang C-J, Xiang D-X, Xiong X-M, et al. Inhibitory effect of
554 resveratrol derivative BTM-0512 on high glucose-induced cell senescence involves
555 dimethylaminohydrolase/asymmetric dimethylarginine pathway. *Clin Exp Pharmacol Physiol*.
556 2010;37: 630–635. doi:10.1111/j.1440-1681.2010.05368.x
- 557 38. Yh D, D A, Hq H, N W, N Y, Yt W, et al. Inhibition of TNF- α -mediated endothelial cell-
558 monocyte cell adhesion and adhesion molecules expression by the resveratrol derivative, trans-
559 3,5,4'-trimethoxystilbene. In: *Phytotherapy research : PTR* [Internet]. Mar 2011 [cited 15 Feb
560 2021]. doi:10.1002/ptr.3279
- 561 39. Xi M, Jy Y, Gl C, Lh W, Lj Z, S W, et al. Effects of resveratrol and its derivatives on
562 lipopolysaccharide-induced microglial activation and their structure-activity relationships. In:
563 *Chemico-biological interactions* [Internet]. 7 Oct 2008 [cited 15 Feb 2021].
564 doi:10.1016/j.cbi.2008.04.015

- 565 40. Effects of resveratrol-related hydroxystilbenes on the nitric oxide production in macrophage
566 cells: structural requirements and mechanism of action. *Life Sci.* 2002;71: 2071–2082.
567 doi:10.1016/S0024-3205(02)01971-9
- 568 41. Farzaei MH, Abdollahi M, Rahimi R. Role of dietary polyphenols in the management of peptic
569 ulcer. *World J Gastroenterol.* 2015;21: 6499–6517. doi:10.3748/wjg.v21.i21.6499
- 570 42. Sholler GLS, Brard L, Straub JA, Dorf L, Illyene S, Koto K, et al. Nifurtimox Induces Apoptosis
571 of Neuroblastoma Cells in vitro and in vivo. *J Pediatr Hematol Oncol.* 2009;31: 187–193.
572 doi:10.1097/MPH.0b013e3181984d91
- 573 43. Du M, Zhang L, Scorsone KA, Woodfield SE, Zage PE. Nifurtimox Is Effective Against Neural
574 Tumor Cells and Is Synergistic with Buthionine Sulfoximine. *Sci Rep.* 2016;6: 27458.
575 doi:10.1038/srep27458
- 576 44. Koto KS, Lescault P, Brard L, Kim K, Singh RK, Bond J, et al. Antitumor activity of nifurtimox
577 is enhanced with tetrathiomolybdate in medulloblastoma. *Int J Oncol.* 2011;38: 1329–1341.
578 doi:10.3892/ijo.2011.971
- 579 45. Goldshmidt H, Matas D, Kabi A, Carmi S, Hope R, Michaeli S. Persistent ER stress induces the
580 spliced leader RNA silencing pathway (SLS), leading to programmed cell death in *Trypanosoma*
581 *brucei*. *PLoS Pathog.* 2010;6: e1000731. doi:10.1371/journal.ppat.1000731
- 582 46. Uzcátegui NL, Carmona-Gutiérrez D, Denninger V, Schoenfeld C, Lang F, Figarella K, et al.
583 Antiproliferative effect of dihydroxyacetone on *Trypanosoma brucei* bloodstream forms: cell
584 cycle progression, subcellular alterations, and cell death. *Antimicrob Agents Chemother.*
585 2007;51: 3960–3968. doi:10.1128/AAC.00423-07
- 586 47. Delgado M, Anderson P, Garcia-Salcedo JA, Caro M, Gonzalez-Rey E. Neuropeptides kill
587 African trypanosomes by targeting intracellular compartments and inducing autophagic-like cell
588 death. *Cell Death Differ.* 2009;16: 406–416. doi:10.1038/cdd.2008.161
- 589 48. Lim KT, Yeoh CY, Zainuddin Z, Ilham Adenan M. (+)-Spectraline and Iso-6-Spectraline Induce
590 a Possible Cross-Talk between Autophagy and Apoptosis in *Trypanosoma brucei rhodesiense*.
591 *Trop Med Infect Dis.* 2019;4. doi:10.3390/tropicalmed4030098
- 592 49. Ojha R, Ishaq M, Singh SK. Caspase-mediated crosstalk between autophagy and apoptosis:
593 Mutual adjustment or matter of dominance. *J Cancer Res Ther.* 2015;11: 514–524.
594 doi:10.4103/0973-1482.163695
- 595 50. Acharya BR, Bhattacharyya S, Choudhury D, Chakrabarti G. The microtubule depolymerizing
596 agent naphthazarin induces both apoptosis and autophagy in A549 lung cancer cells. *Apoptosis*
597 *Int J Program Cell Death.* 2011;16: 924–939. doi:10.1007/s10495-011-0613-1
- 598 51. Reunanen H, Marttinen M, Hirsimäki P. Effects of griseofulvin and nocodazole on the
599 accumulation of autophagic vacuoles in Ehrlich ascites tumor cells. *Exp Mol Pathol.* 1988;48:
600 97–102. doi:10.1016/0014-4800(88)90048-2
- 601 52. Kuo P-L, Hsu Y-L, Cho C-Y. Plumbagin induces G2-M arrest and autophagy by inhibiting the
602 AKT/mammalian target of rapamycin pathway in breast cancer cells. *Mol Cancer Ther.* 2006;5:
603 3209–3221. doi:10.1158/1535-7163.MCT-06-0478
- 604 53. Kondo Y, Kanzawa T, Sawaya R, Kondo S. The role of autophagy in cancer development and
605 response to therapy. *Nat Rev Cancer.* 2005;5: 726–734. doi:10.1038/nrc1692

- 606 54. Yu J, Nagasu H, Murakami T, Hoang H, Broderick L, Hoffman HM, et al. Inflammasome
607 activation leads to Caspase-1-dependent mitochondrial damage and block of mitophagy. Proc
608 Natl Acad Sci U S A. 2014;111: 15514–15519. doi:10.1073/pnas.1414859111
- 609 55. Richard M. Locksley Seymour J. Klebanoff. Oxygen-dependent microbicidal systems of
610 phagocytes and host defense against intracellular protozoa - Locksley - 1983 - Journal of
611 Cellular Biochemistry - Wiley Online Library. [cited 2 Feb 2021]. Available:
612 <https://onlinelibrary.wiley.com/doi/abs/10.1002/jcb.240220306>
- 613 56. Nathan C, Nogueira N, Juangbhanich C, Ellis J, Cohn Z. Activation of macrophages in vivo and
614 in vitro. Correlation between hydrogen peroxide release and killing of *Trypanosoma cruzi*. J
615 Exp Med. 1979;149: 1056–1068. doi:10.1084/jem.149.5.1056
- 616

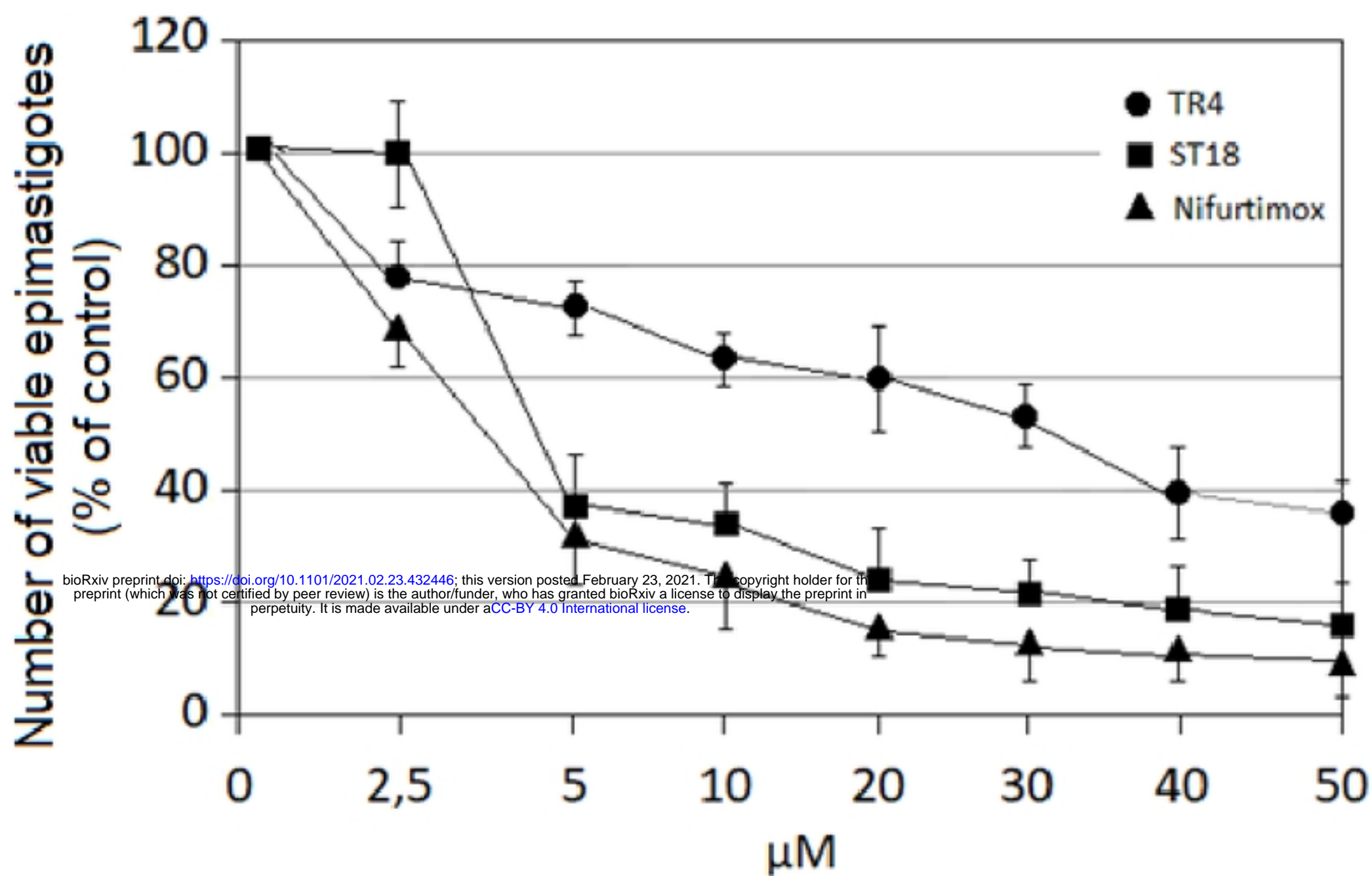
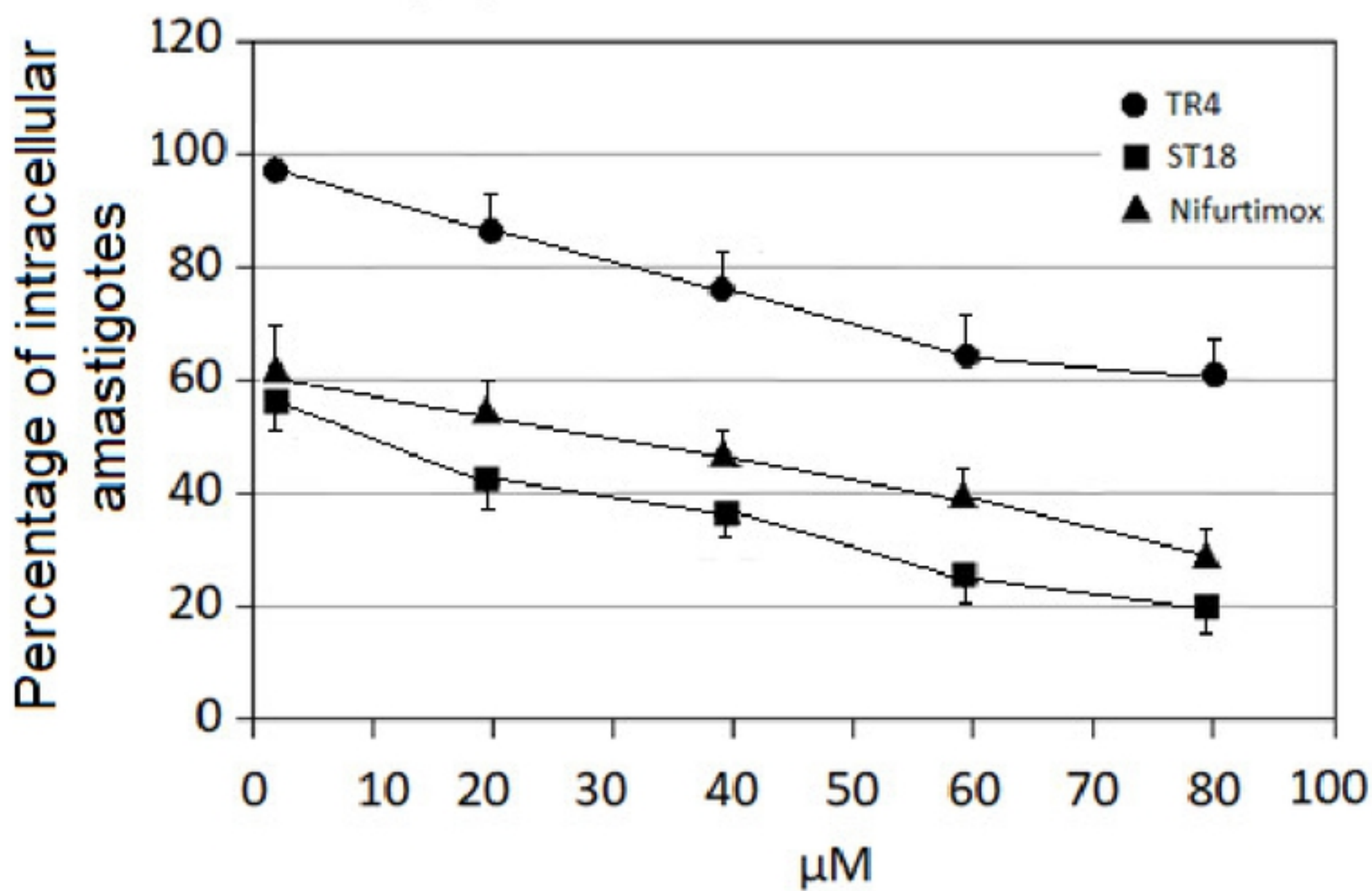
A**B**

Figure 1

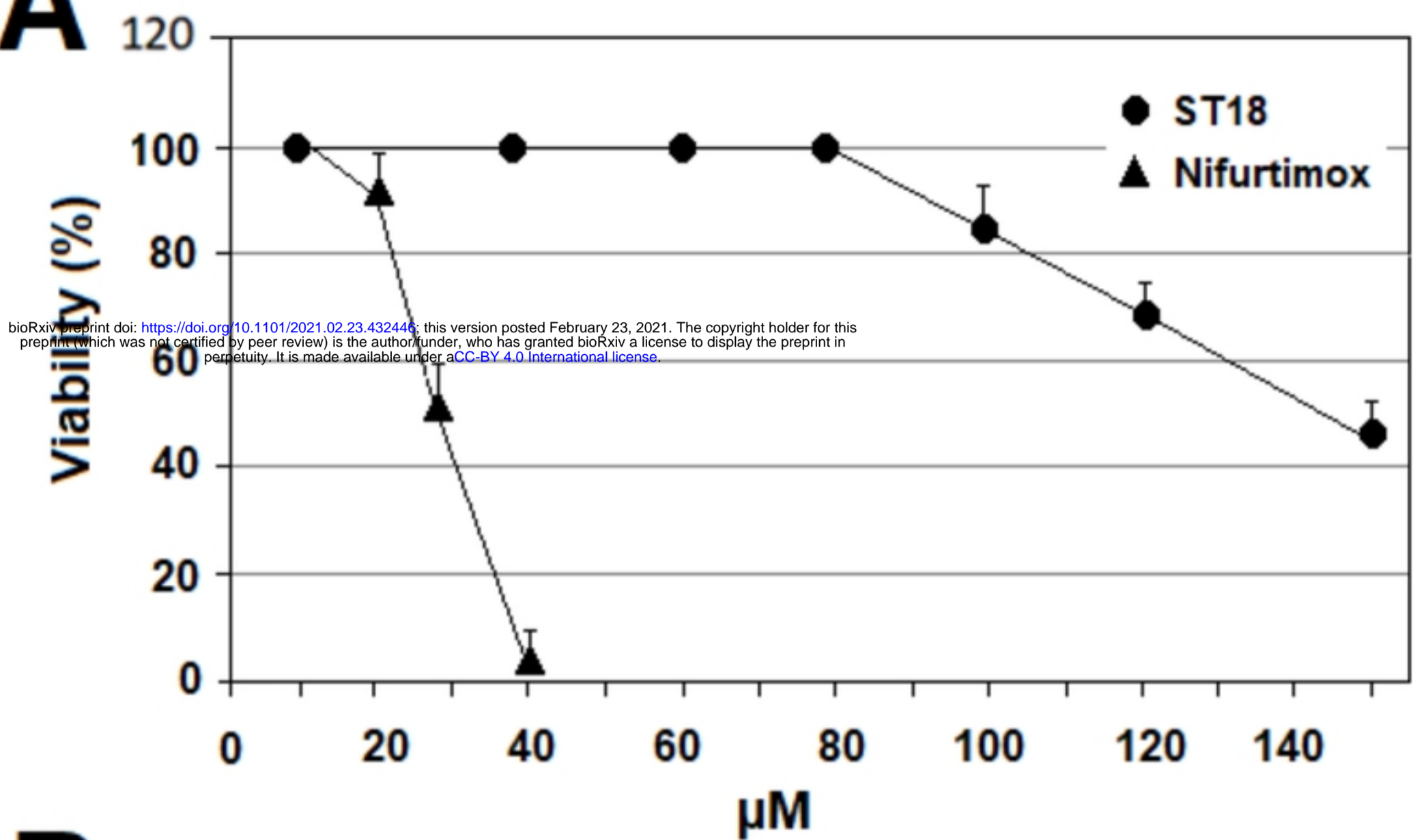
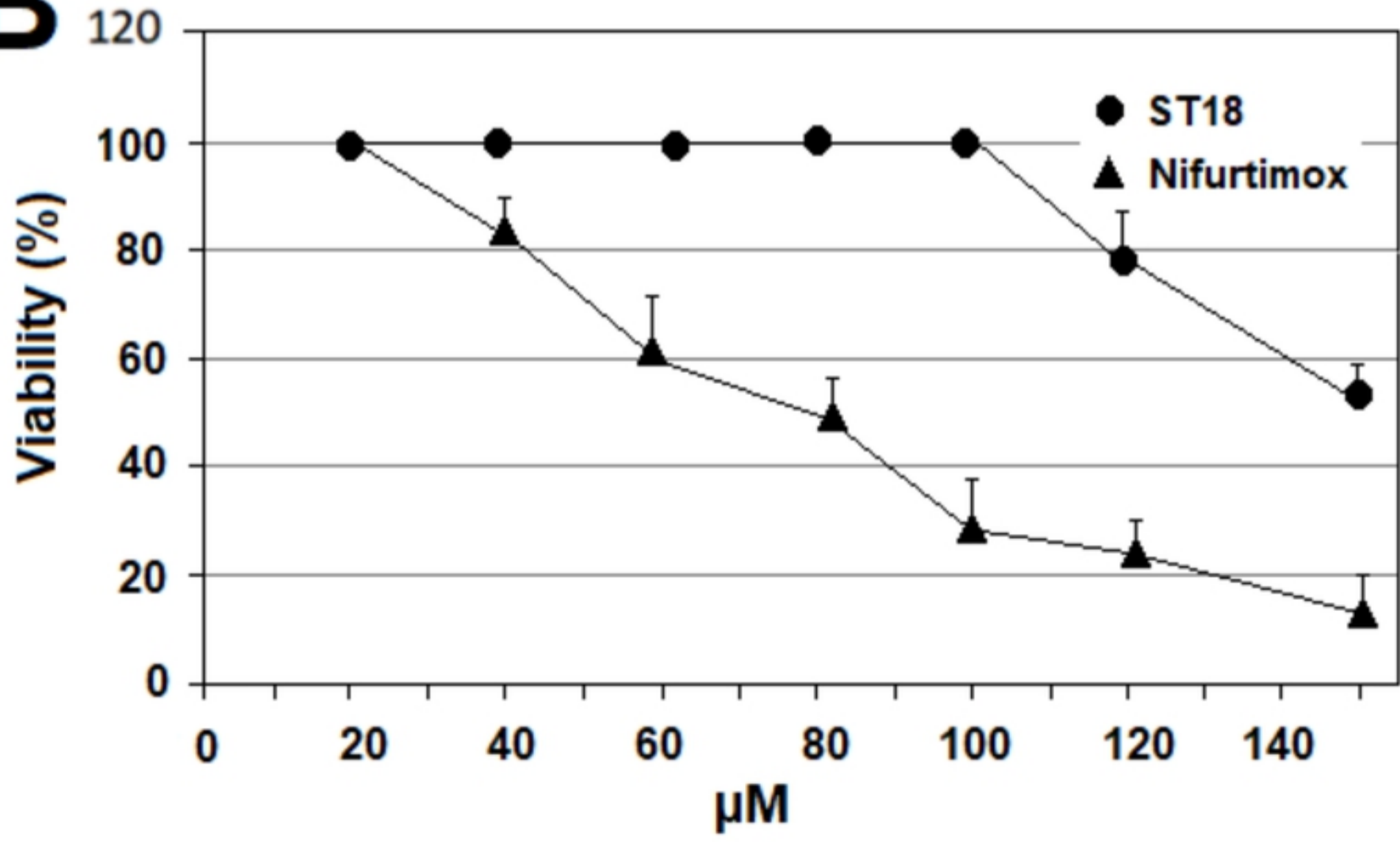
A**B**

Figure 2

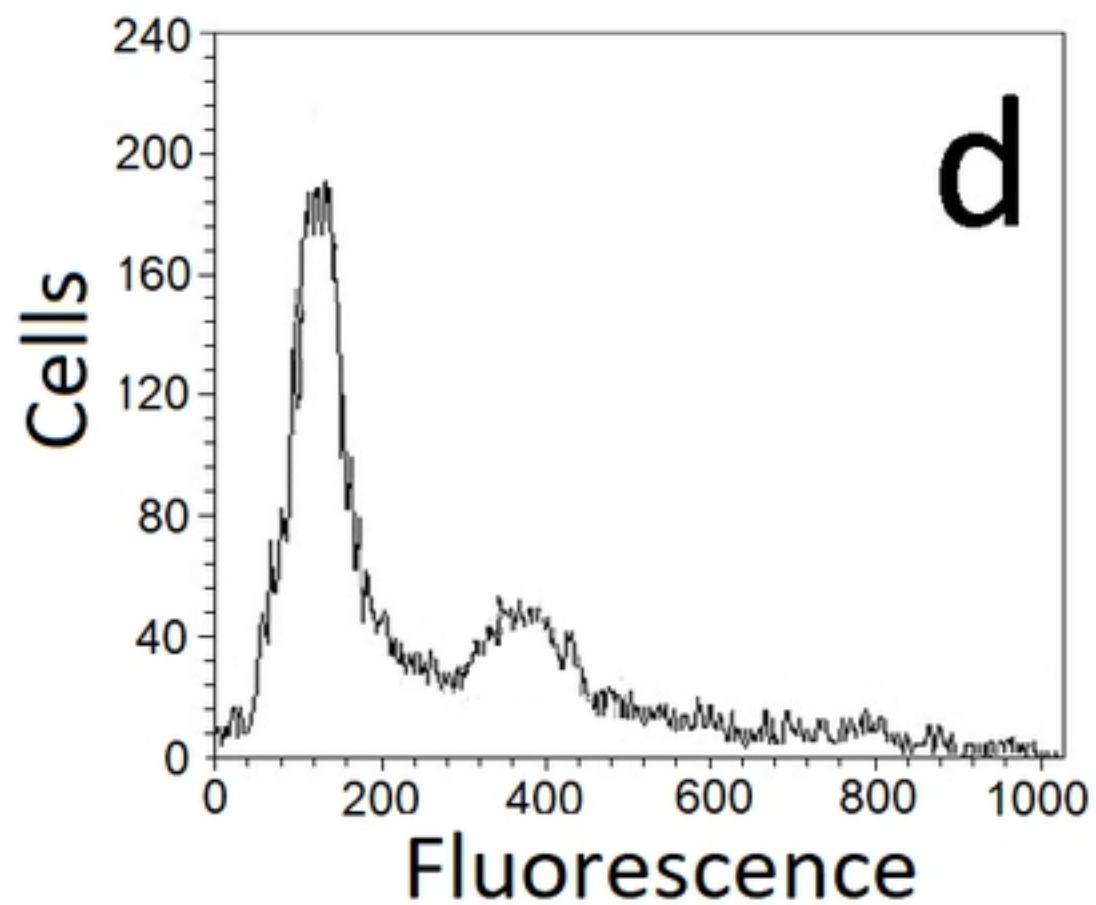
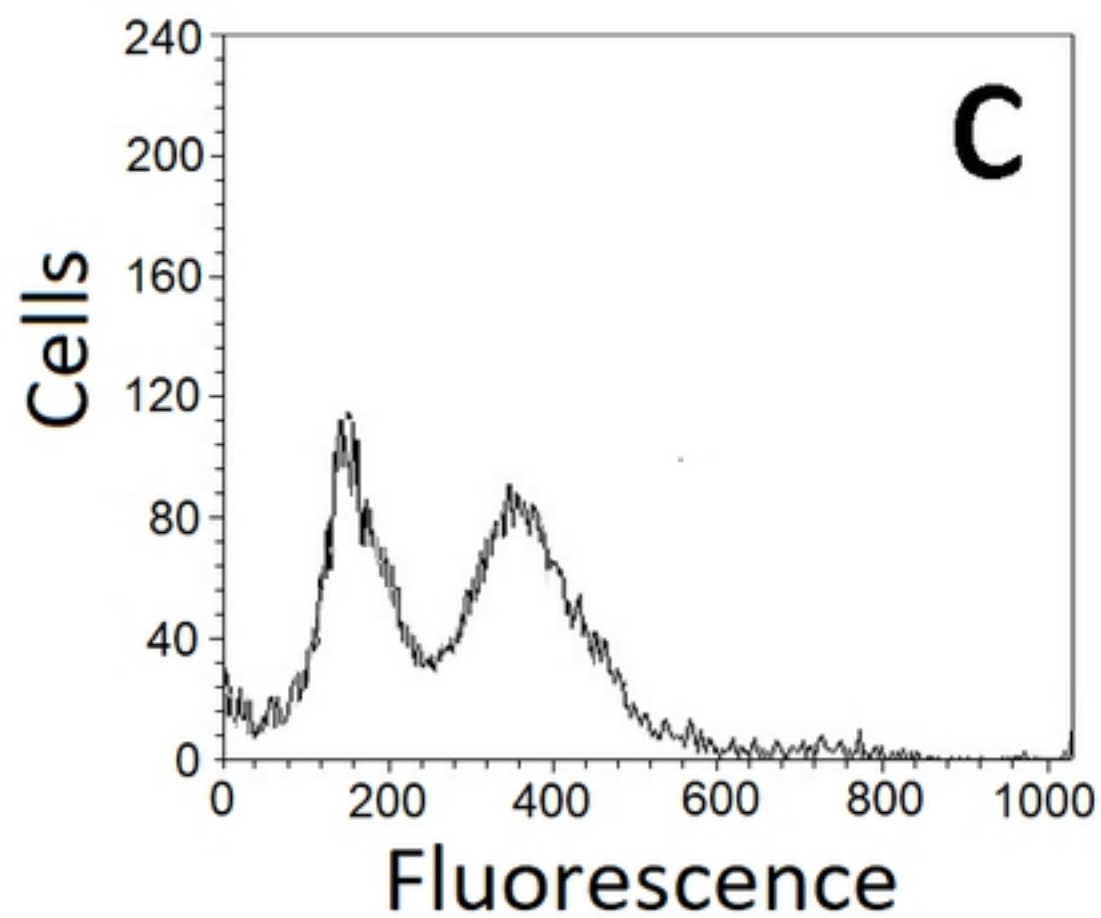
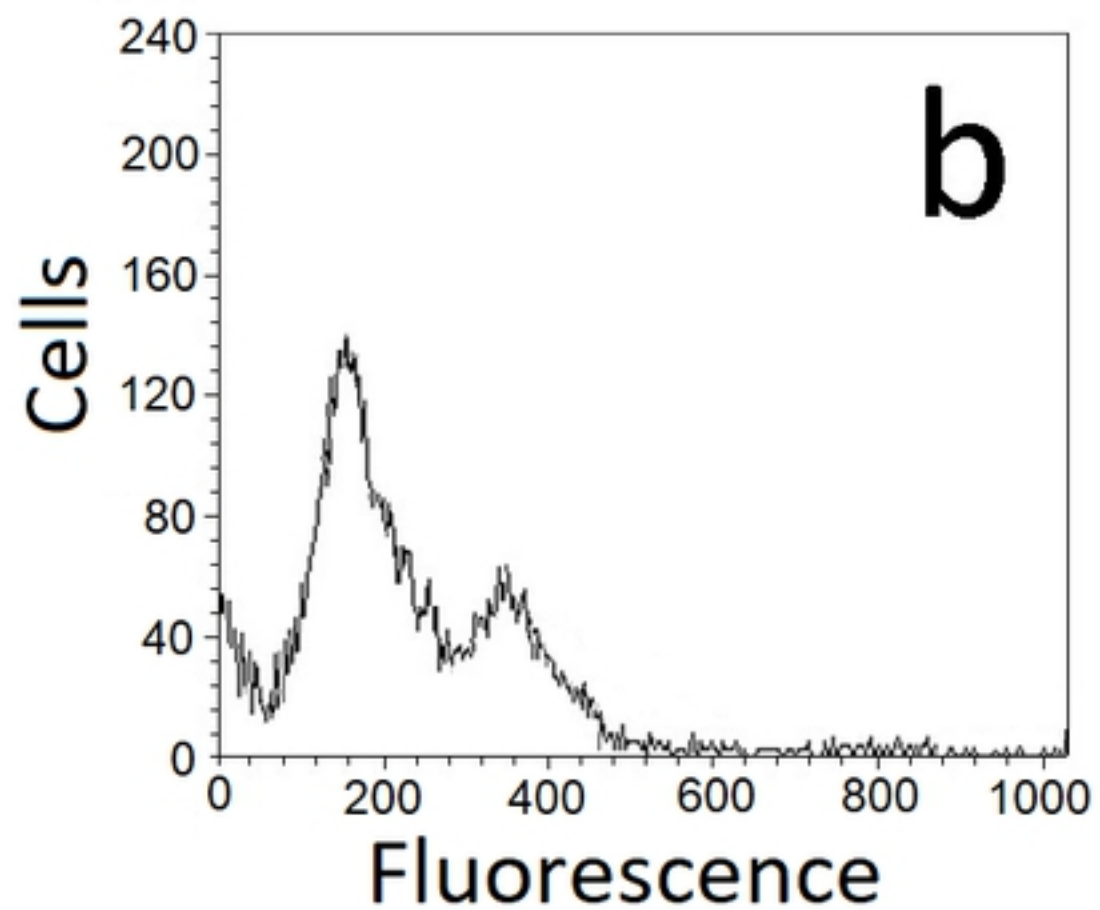
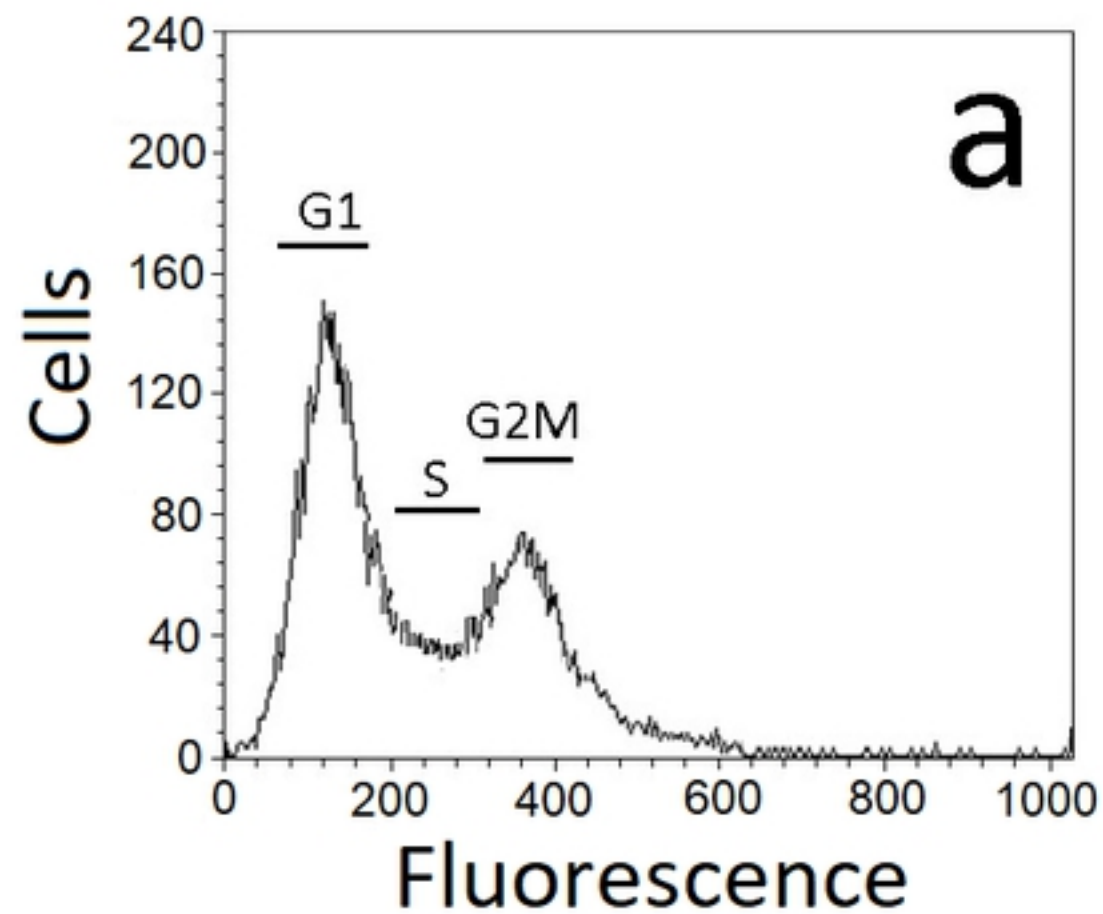


Figure 3

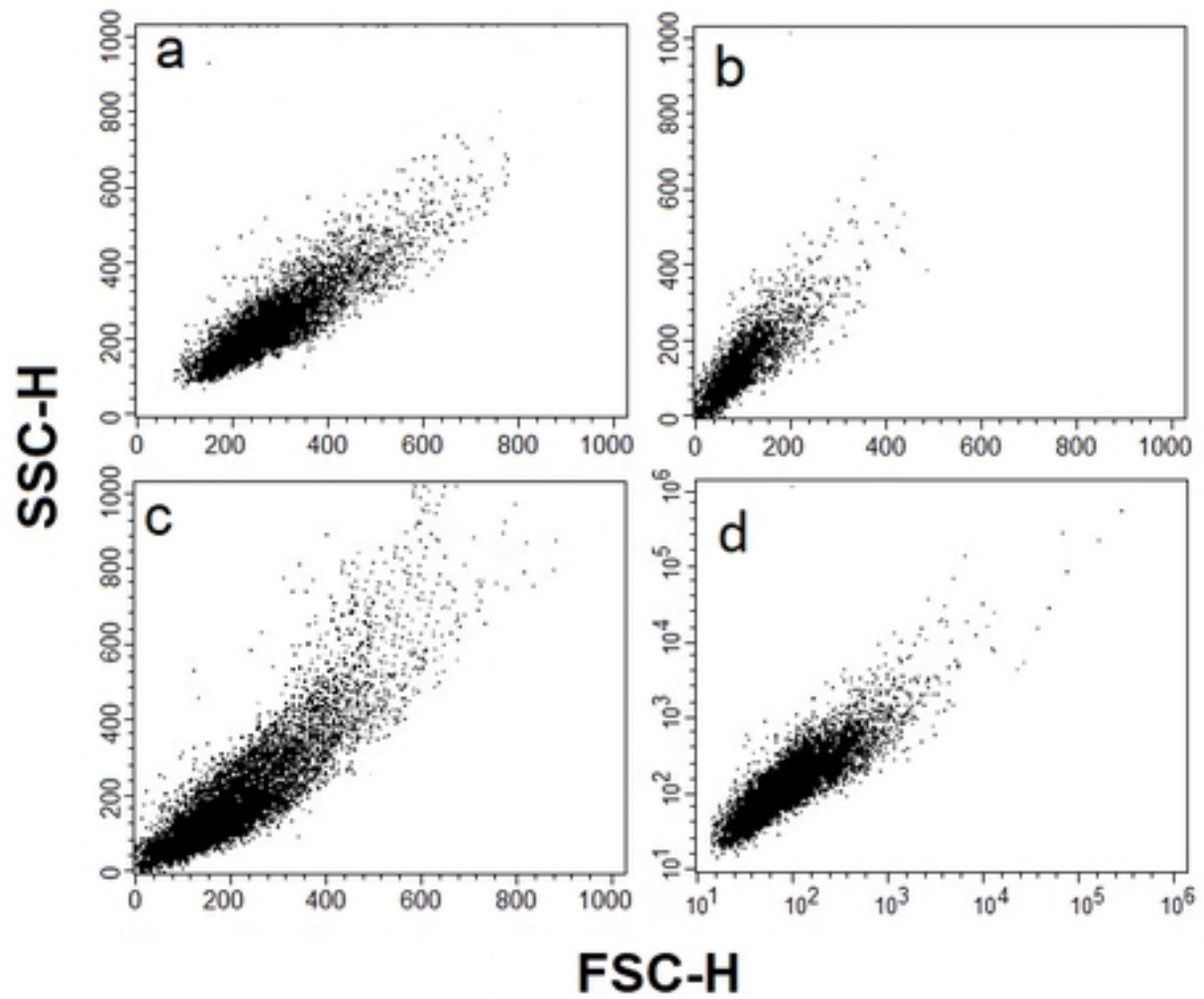
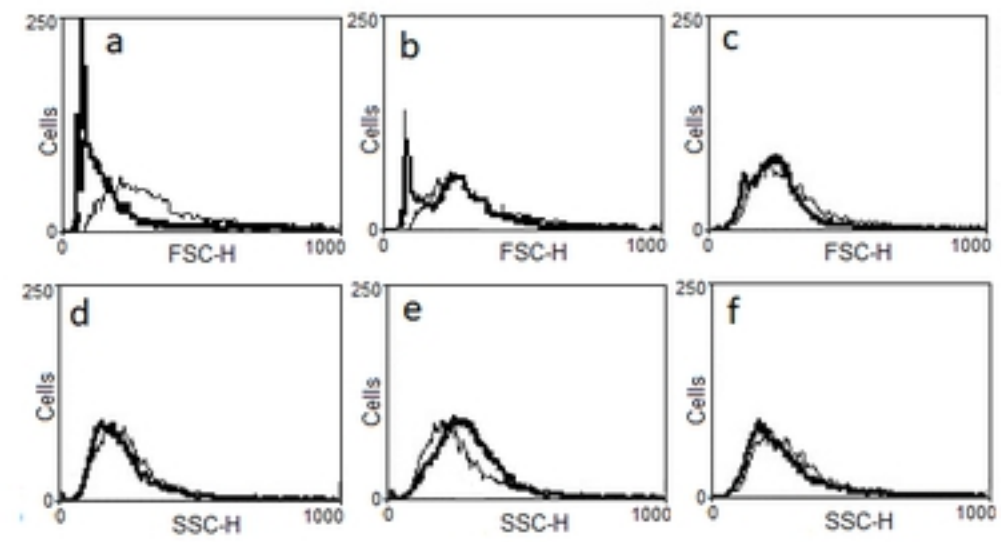
A**B**

Figure 4

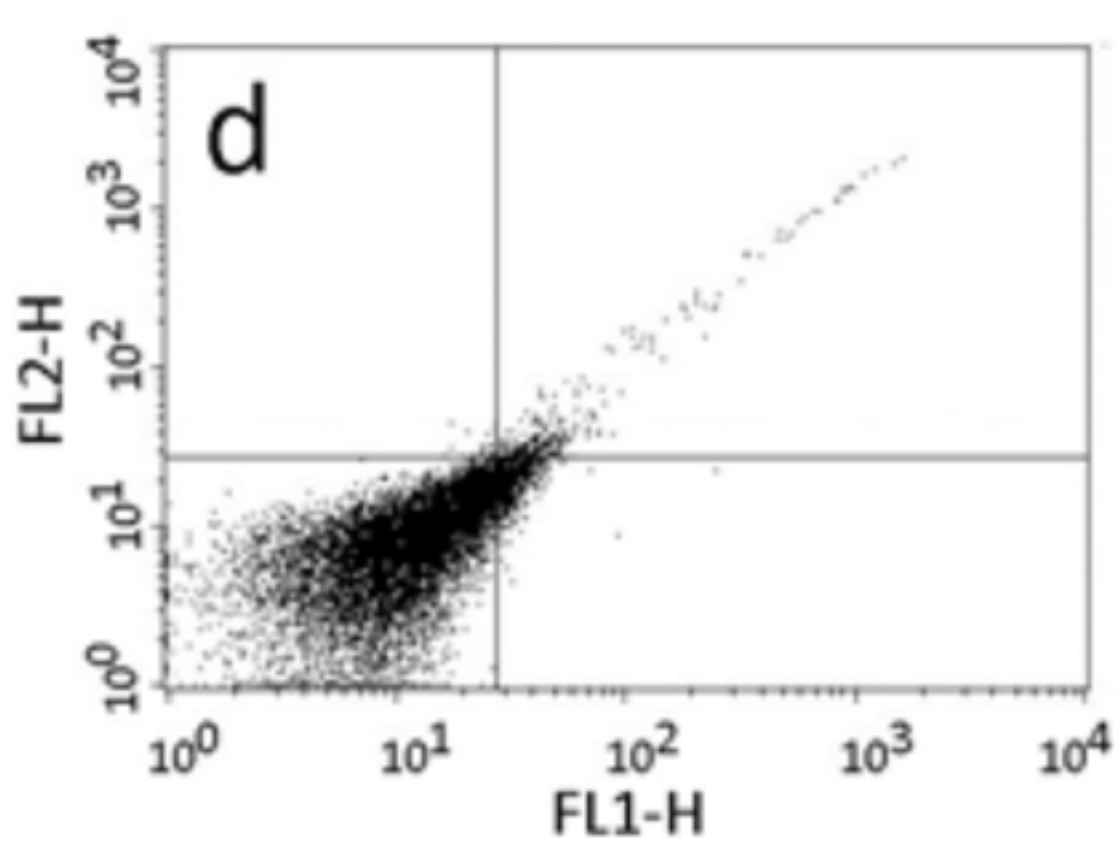
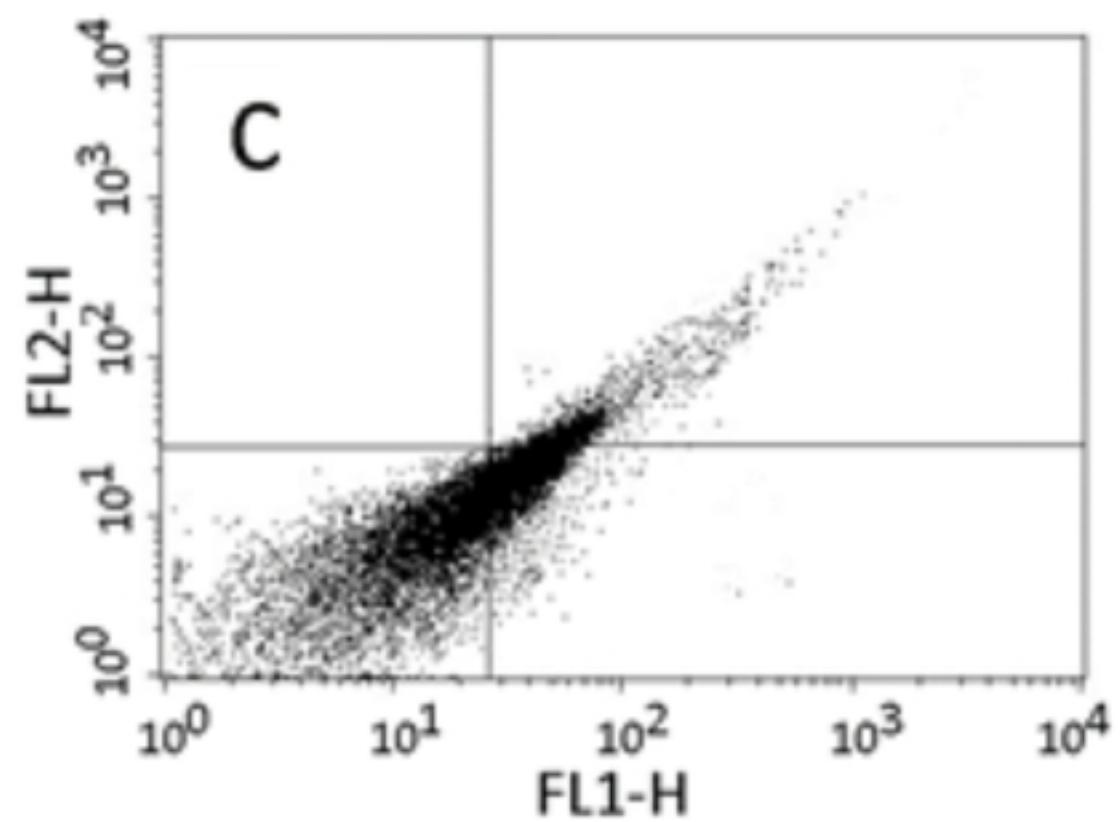
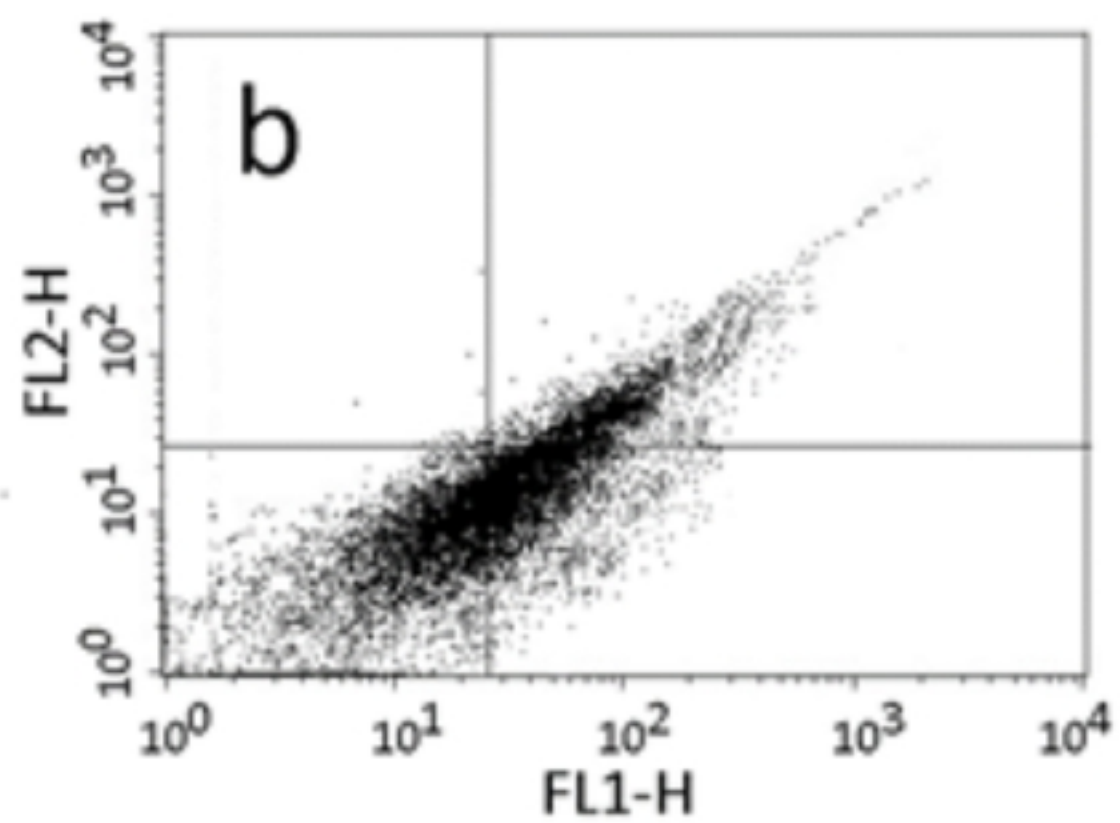
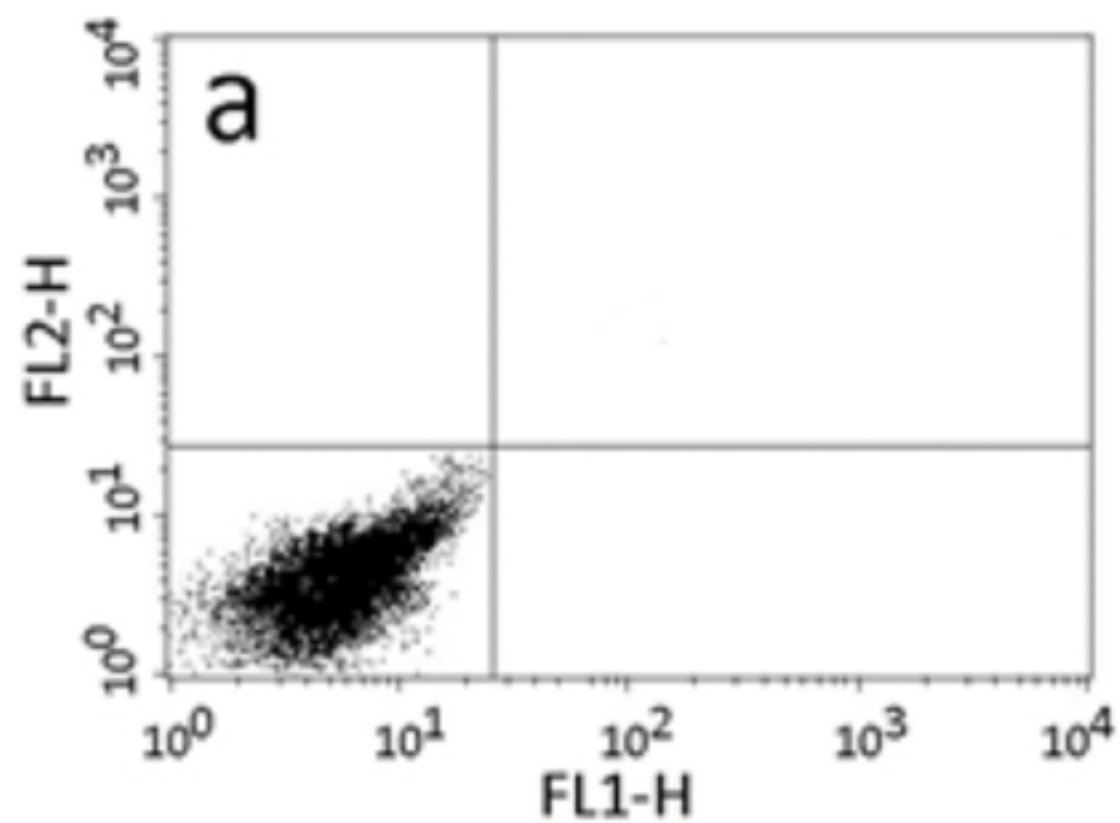


Figure 5

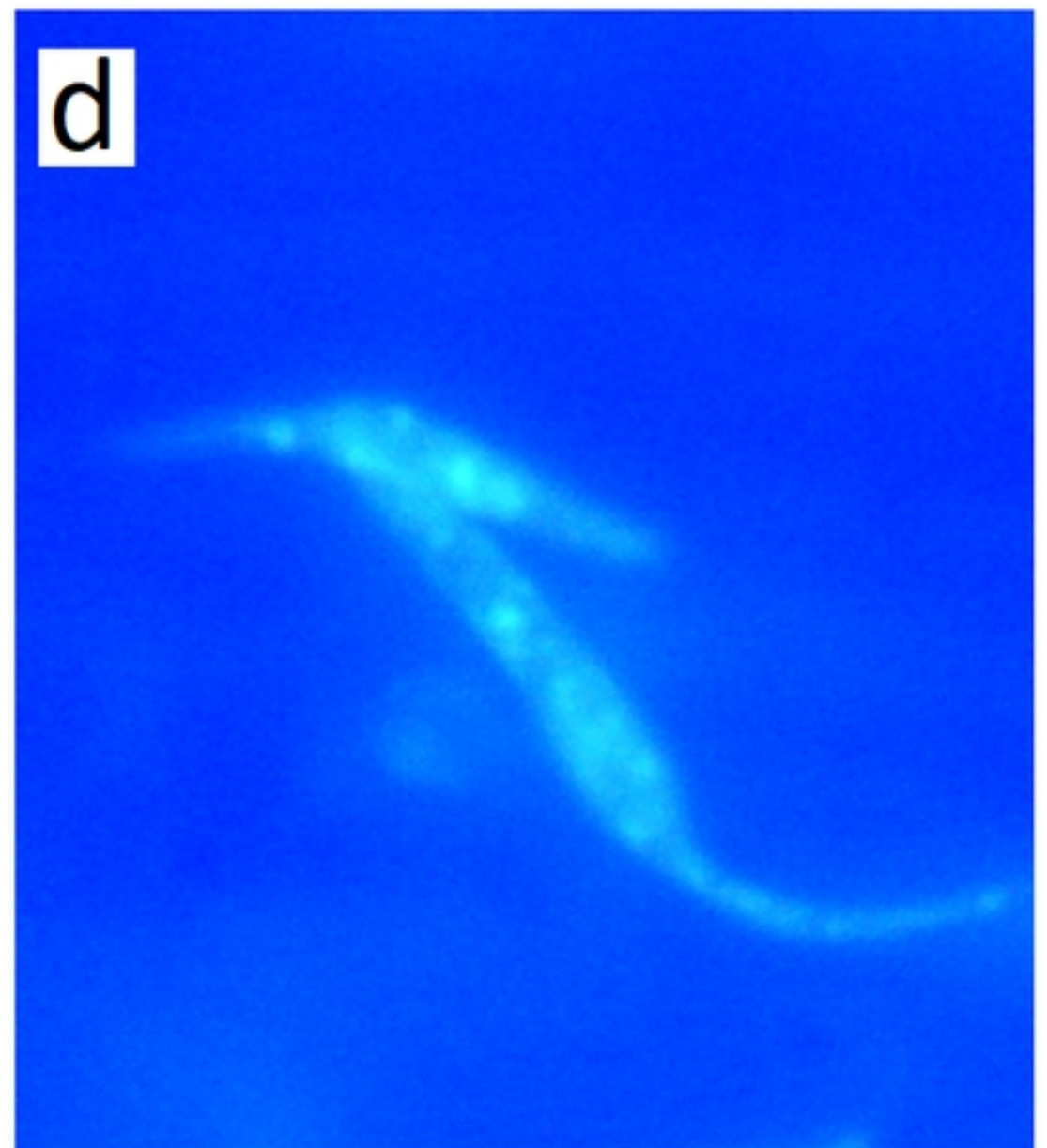
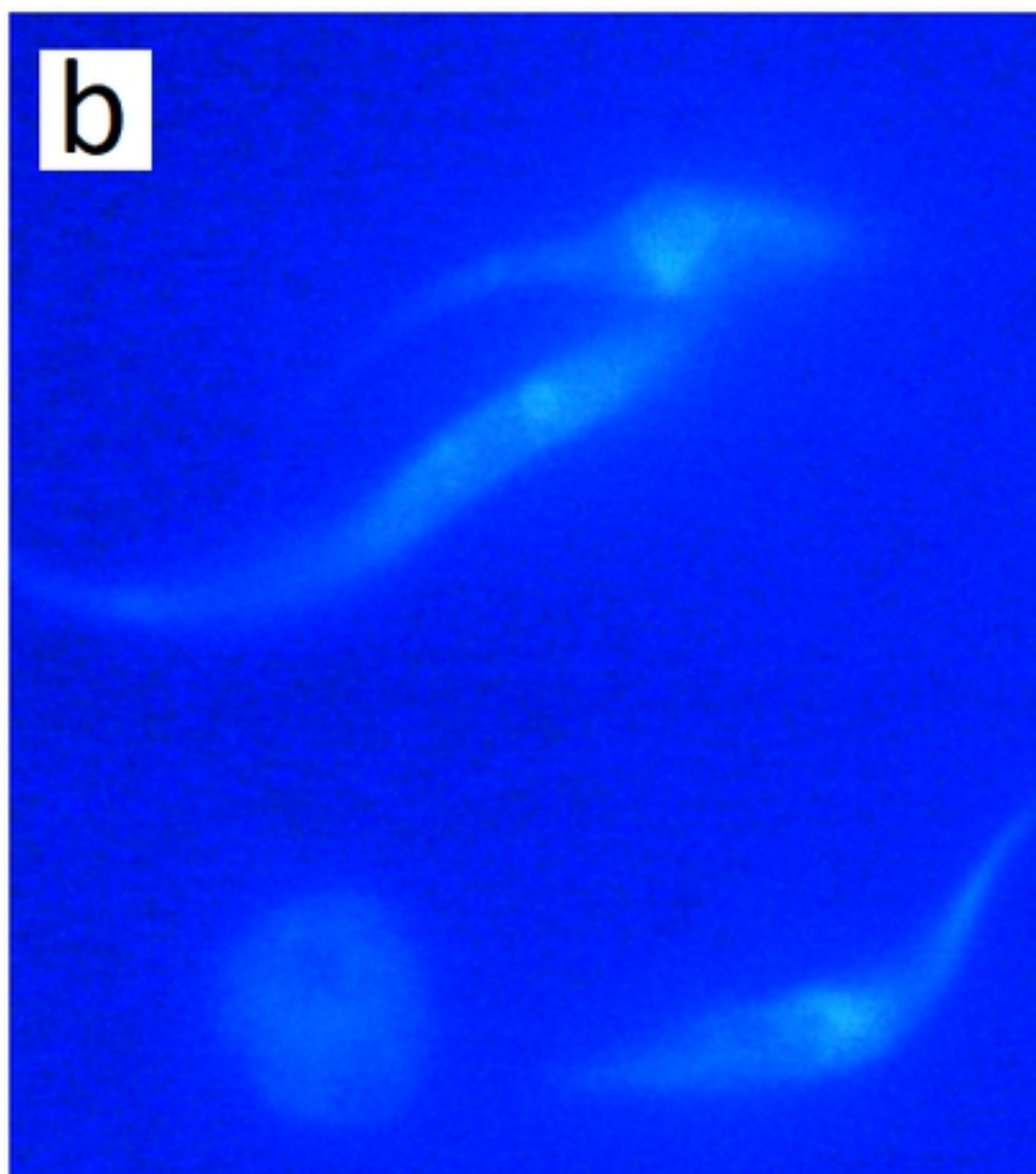
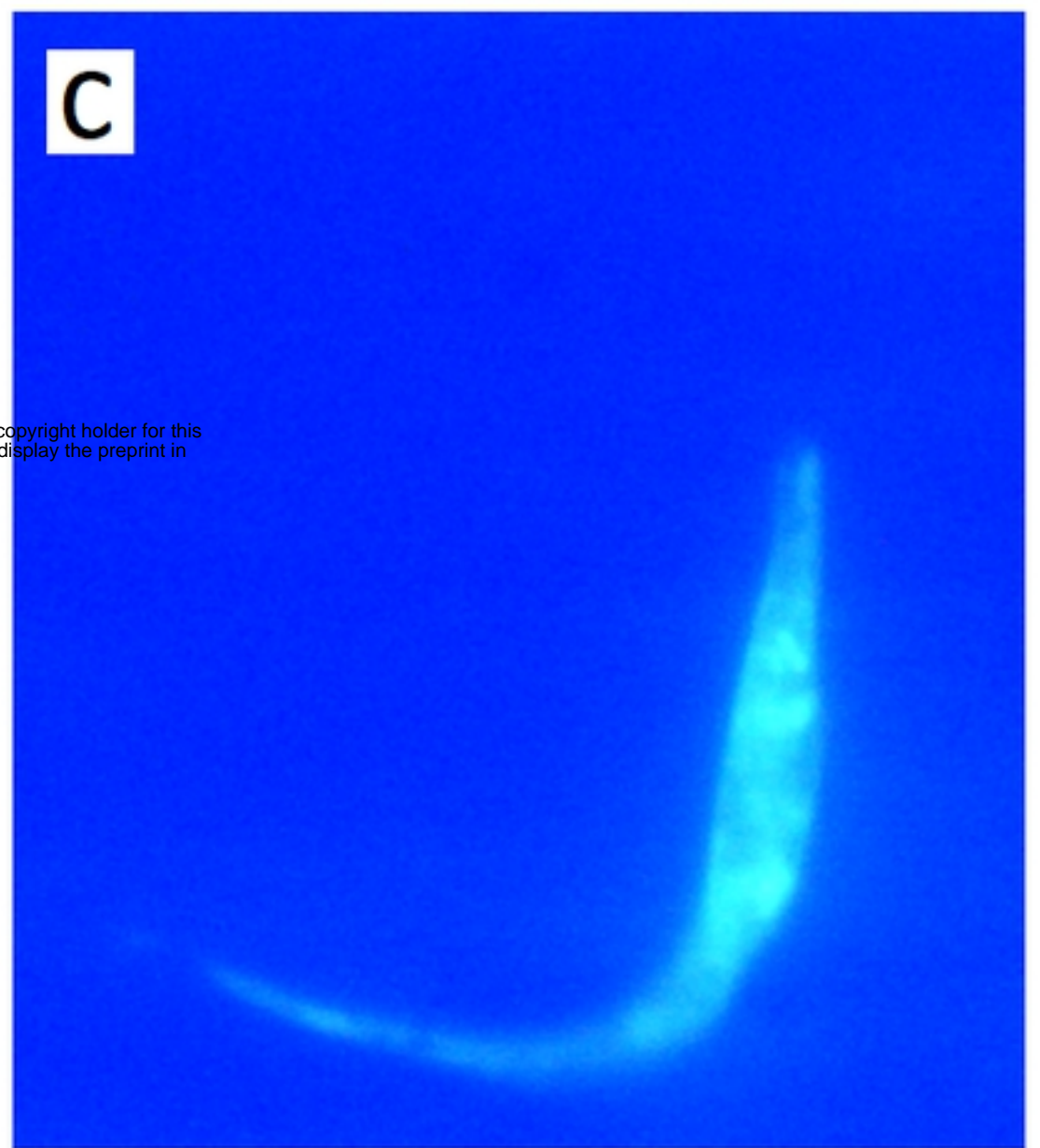
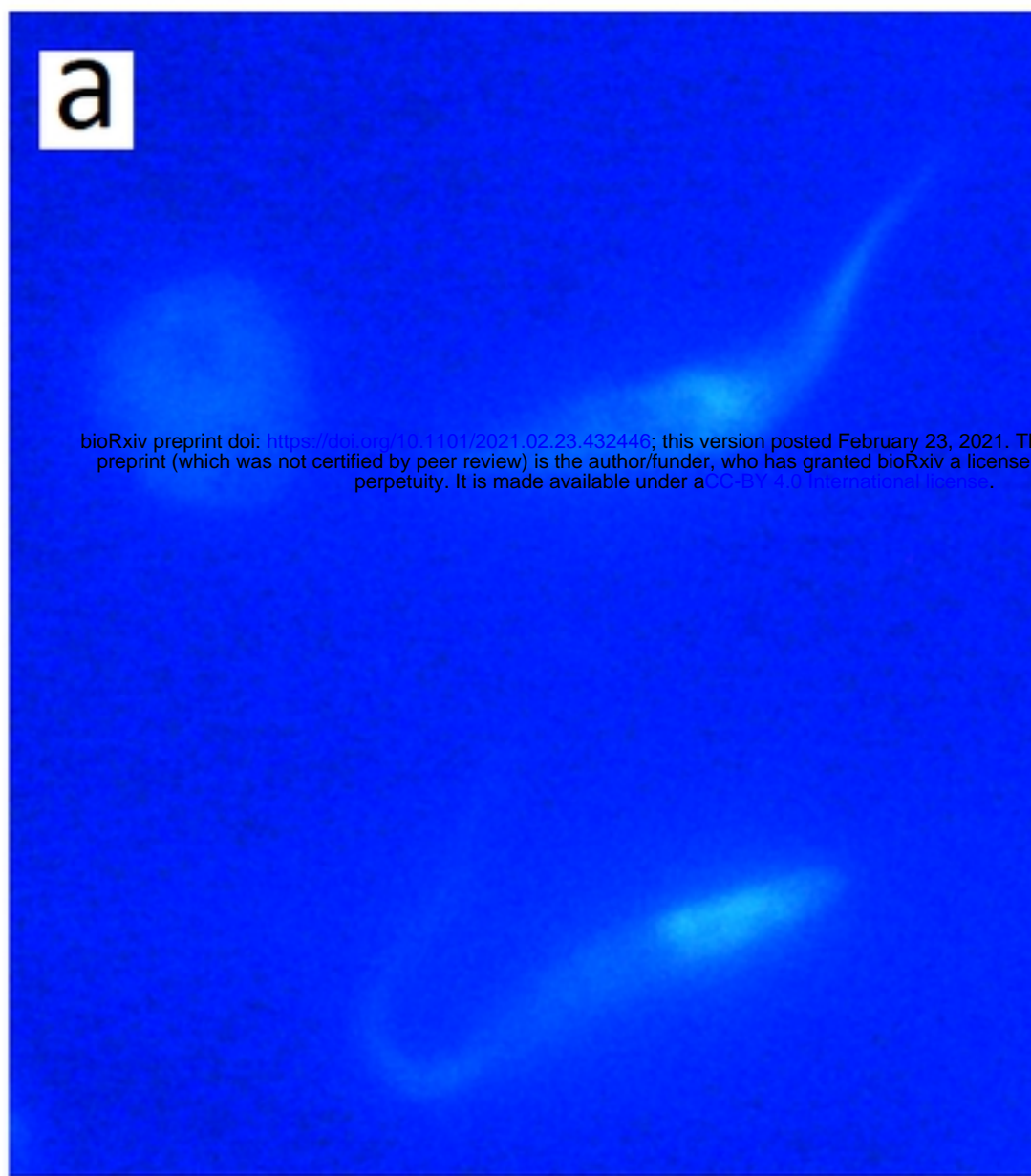


Figure 6

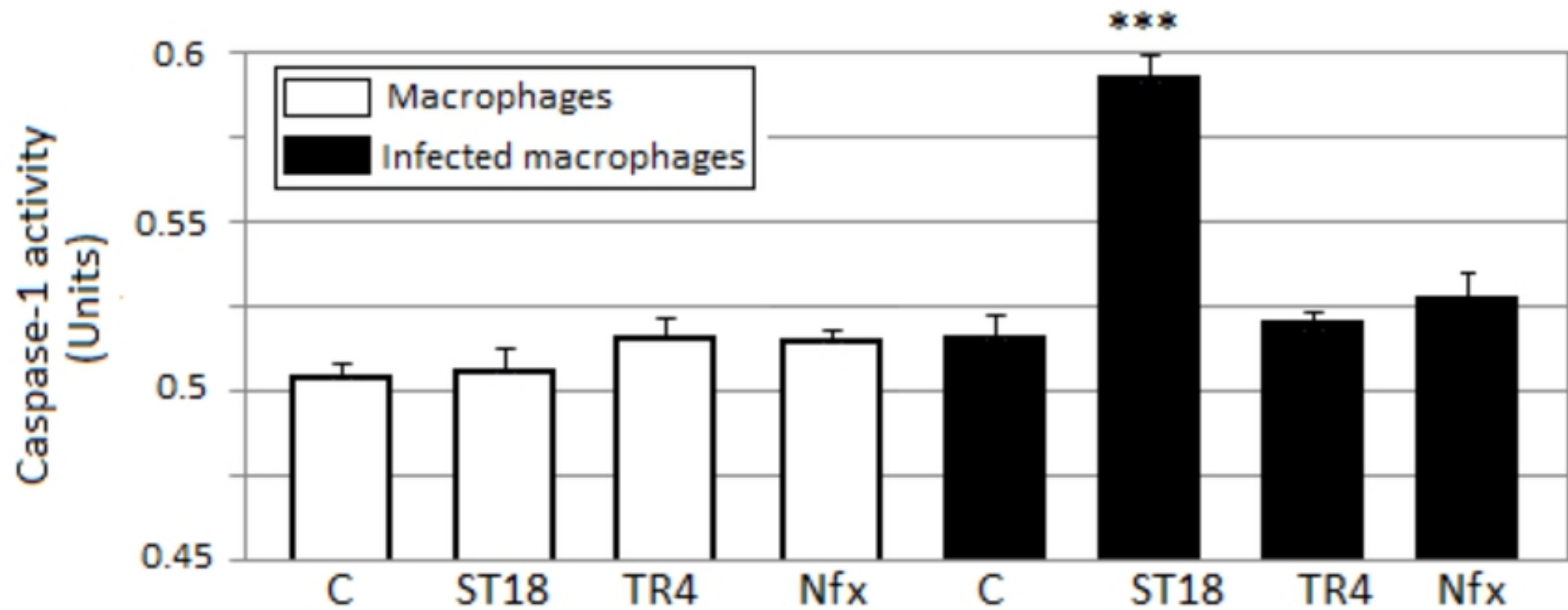


Figure 7